nature cell biology

Hippo signalling governs cytosolic nucleic acid sensing through YAP/TAZ-mediated TBK1 blockade

Qian Zhang[1,7], Fansen Meng[1,7], Shasha Chen[1], Steven W. Plouffe[2], Shiying Wu[1], Shengduo Liu[1], Xinran Li[1], Ruyuan Zhou[1], Junxian Wang[1], Bin Zhao[1], Jianming Liu[3], Jun Qin[4], Jian Zou[5], Xin-Hua Feng[1,6], Kun-Liang Guan[2] and Pinglong Xu[1,8]

The Hippo pathway senses cellular conditions and regulates YAP/TAZ to control cellular and tissue homeostasis, while TBK1 is central for cytosolic nucleic acid sensing and antiviral defence. The correlation between cellular nutrient/physical status and host antiviral defence is interesting but not well understood. Here we find that YAP/TAZ act as natural inhibitors of TBK1 and are vital for antiviral physiology. Independent of transcriptional regulation and through the transactivation domain, YAP/TAZ associate directly with TBK1 and abolish virus-induced TBK1 activation, by preventing TBK1 Lys63-linked ubiquitylation and the binding of adaptors/substrates. Accordingly, YAP/TAZ deletion/depletion or cellular conditions inactivating YAP/TAZ through Lats1/2 kinases relieve TBK1 suppression and boost antiviral responses, whereas expression of the transcriptionally inactive YAP dampens cytosolic RNA/DNA sensing and weakens the antiviral defence in cells and zebrafish. Thus, we describe a function of YAP/TAZ and the Hippo pathway in innate immunity, by linking cellular nutrient/physical status to antiviral host defence.

Metazoans use innate defence mechanisms to recognize conserved pathogen-associated molecular patterns and fight against pathogen infections. Cytosolic nucleic acid sensors are crucial components of the defence system in vertebrates, particularly for detecting viruses that have breached physical barriers and been replicated within the cell. Viral double-stranded RNA is detected in the cytosol by RIG-I-like receptors[1,2], while viral DNA is recognized by cytosolic sensors including cGAS[3–6], IFI16, DDX41 and others[7]. Facilitated by mitochondrial-associated MAVS (also known as VISA, IPS-1 or Cardif) or endoplasmic reticulum-located STING (also known as ERIS, MITA, MPYS or TMEM173), viral nucleic acid recognition leads to the activation of TBK1 and/or IKKε kinases that phosphorylate and mobilize IRF3, which then dimerizes and translocates to the nucleus, where it acts as a DNA-binding transcription factor[8,9]. Assembly of the MAVS or STING signalling complex also induces NF-κB activation[10,11], which cooperates with IRF3 to drive the expression of type I and III interferons. The antiviral defence of the self and neighbouring cells is thus established by coordinating a large number of interferon-stimulated genes (ISGs) through classical JAK–STAT signalling, to clear/prevent viral infection and modulate adaptive immunity[12,13].

How cytosolic nucleic acid sensing is affected by cellular conditions, such as nutrient/energy stress or cell–cell contact, is an interesting question that remains to be answered. Self-association of MAVS or STING molecules initiates the recruitment of TRAFs, TBK1/IKKε and IRF3[14], where intermolecular *trans*-phosphorylation, facilitated by Lys63-linked ubiquitylation and adaptor-driven association, leads to TBK1/IKKε activation[15]. Viral-induced TBK1 activation is a slow process subject to complex regulations involving interacting proteins and post-translational modifications[16–18], including ion metal phosphatase PPM1A[19] and kinase Mst1[20]. Conversely, aberrant reactions to own nucleic acids and subsequent IFN production trigger autoimmune and autoinflammatory diseases[21,22]; thus, the activation of TBK1 requires strict regulation. TBK1 and IKKε also serve as key regulators of apoptosis, autophagy and inflammatory responses[23–25] and act as important inducers to drive tumorigenesis[26,27]. Nevertheless, the regulatory mechanism for TBK1/IKKε activation and termination is largely unknown.

The Hippo pathway was originally discovered in *Drosophila* and is highly conserved[28–31]. The transcription co-activators YAP and TAZ are the downstream effectors, which are regulated by the Lats1/2

[1]Life Sciences Institute and Innovation Center for Cell Signaling Network, Zhejiang University, Hangzhou 310058, China. [2]Department of Pharmacology and Moores Cancer Center, University of California San Diego, La Jolla, California 92093, USA. [3]Department of Cardiology, Boston Children's Hospital, Harvard Medical School, Boston, Massachusetts 02115, USA. [4]The Key Laboratory of Stem Cell Biology, Chinese Academy of Sciences Center for Excellence in Molecular Cell Science, Institute of Health Sciences, Shanghai Institutes for Biological Sciences, Chinese Academy of Sciences, Shanghai 200031, China. [5]Eye Center of the Second Affiliated Hospital School of Medicine, Institutes of Translational Medicine, Zhejiang University, Hangzhou 310058, China. [6]Michael E. DeBakey Department of Surgery and Department of Molecular and Cellular Biology, Baylor College of Medicine, Houston, Texas 77030, USA. [7]These authors contributed equally to this work.
[8]Correspondence should be addressed to P.X. (e-mail: xupl@zju.edu.cn)

Received 9 November 2016; accepted 22 February 2017; published online 27 March 2017; DOI: 10.1038/ncb3496

kinases in response to unfavourable growth conditions to retain YAP/TAZ in the cytoplasm for ubiquitylation and degradation[32,33]. Otherwise, YAP/TAZ are localized in the nucleus to bind to and activate the TEAD family transcription factors to transcribe target genes promoting cell proliferation, migration and survival[34]. How the Hippo pathway cooperates with other signalling pathways to regulate a variety of physiological processes, such as host defence, is largely unanswered. Regulation of YAP/TAZ is very complex and can be affected via crosstalk with the WNT pathway[35], G-protein-coupled receptor (GPCR) signalling[36–39], and the transforming growth factor-β (TGF-β)[40] and Notch pathways[41]. Both Hippo and cytosolic nucleic acid sensing are ancient and evolutionally highly conserved pathways and are present in all vertebrates. The opposing biological processes, such as growth and survival governed by YAP/TAZ and danger sensing controlled by TBK1, indicate that these factors may influence each other. One group recently reported an intriguing crosstalk between the Hippo pathway and Toll-like receptor signalling in *Drosophila* through Yorkie-mediated induction of the IκB homologue Cactus[42]. The finding indicates an integral role for YAP/TAZ in anti-bacterial host defence in invertebrates.

Here we find that key components of antiviral defence, the TBK1/IKKε kinases, are directly suppressed by YAP/TAZ independent of their transcriptional potential. YAP/TAZ associate with TBK1 and prevent its Lys63 ubiquitylation and adaptor/substrate association. Accordingly, YAP/TAZ knockout (KO) or knockdown, or cellular conditions activating Hippo signalling, relieves TBK1 inhibition and boosts the antiviral resistance. Conversely, a transcriptionally inactive YAP mutant can sensitize cells and zebrafish to virus attack. This work reveals an unexpected function of YAP/TAZ and the Hippo pathway in cytosolic nucleic acid sensing and innate antiviral immunity.

RESULTS

Cellular conditions activating Hippo signalling boost cytosolic RNA/DNA sensing

Understanding the regulation of host antiviral immunity by cellular nutrition/physical status is important but has not been systemically studied previously. We first evaluated the level of cellular antiviral signalling following serum starvation by an IRF3-responsive IFN-β reporter. We observed an unanticipated increase in IRF3 transactivation under starvation in response to Sendai virus (SeV) infection (Fig. 1a). Meanwhile we observed an elevated activation of endogenous TBK1 in starved cells following SeV infection, detected by a phospho-Ser172-specific antibody (Fig. 1b, first panel). Likewise, starvation boosted IRF3 transactivation stimulated by ectopic expression of activated RIG-I (caRIG-I) or STING (Fig. 1c,d), but did not significantly potentiate signalling such as Wnt, Hedgehog or TGF-β/Smad (Supplementary Fig. 1A). Serum starvation is known to activate the Hippo pathway[36,37], evidenced by increased YAP Ser127 phosphorylation and TAZ degradation (Fig. 1b). Double deletion of Lats1/2, the upstream kinases of YAP/TAZ, by CRISPR/Cas9 genomic editing[27] abolished both effects in response to cellular nutrient/energy stresses (Supplementary Fig. 1B). Intriguingly, a decrease of IRF3 responsiveness was observed in Lats1/2 double KO (dKO) HEK293A cells, along with the loss of starvation-induced IRF3 transactivation (Fig. 1c,d). This could be partially rescued by reintroduction of Lats1 expression (Fig. 1e). These observations suggest that cellular nutrient status regulates antiviral sensing and it involves the Hippo pathway.

High cell confluence is known to activate Hippo signalling and lead to YAP/TAZ inactivation and degradation[33,43] (Fig. 1f). We thus examined the effect of high cell confluence on IRF3 activation. When stimulated by MAVS, we detected a robust enhancement of IRF3 transactivation in cells at high confluency, which was absent in Lats1/2 dKO cells (Fig. 1g). Likewise, poly(I:C) transfection (TpIC)-induced endogenous IRF3 activation, which simulates cytosolic RNA sensing, was also diminished in Lats1/2 dKO cells (Fig. 1h). Together, these observations verify that the Hippo pathway is a potent regulator of cellular antiviral response.

YAP/TAZ attenuate cytosolic nucleic acid sensing and the antiviral response

YAP/TAZ are Lats1/2 substrates and are key effectors of the Hippo pathway. Since the levels of TAZ protein and/or YAP phosphorylation are associated with the strength of antiviral signalling, we examined the potential effect of YAP/TAZ. Reporter assays with IRF3-responsive IFN-β or ISRE promoter revealed that antiviral responses stimulated by activated RIG-I (caRIG-I) (Fig. 2a,b), STING (Fig. 2c), or TBK1 and IKKε (Supplementary Fig. 2A,B), were all strongly inhibited by ectopic expression of YAP or TAZ in a dose-dependent manner. Similarly, RIG-I-induced IRF3 Ser396 phosphorylation was abolished by YAP co-transfection in a dose-dependent manner (Fig. 2d). Conversely, RIG-I or STING-stimulated IFN-β reporter was significantly higher, when either YAP or TAZ or both were knocked down by short interfering RNA (siRNA) (Fig. 2e,f), similar to MAVS-induced IRF3 transactivation (Supplementary Fig. 2C). We also detected an enhanced TBK1 auto-activation in YAP/TAZ knockdown cells (Supplementary Fig. 2D). All of these observations suggest a negative regulation of YAP/TAZ in antiviral signalling. We observed a similar suppression of YAP/TAZ in the TRIF-stimulated IRF3 transactivation or MyD88-mediated pathway (Supplementary Fig. 2E,F). However, since YAP/TAZ proteins were often at a very low level in a variety of immune cells[44] (Supplementary Fig. 2G), their regulation on TRIF/MyD88 pathways requires further validation.

We subsequently examined endogenous TBK1 activation following VSV infection in HCT 116 colon carcinoma cells, which had short hairpin RNA (shRNA)-mediated knockdown of YAP or TAZ. The shRNA-mediated knockdown was efficient (Fig. 2g), and a marked enhancement of VSV-induced activation of endogenous TBK1 was detected (Fig. 2g), as well as an enhanced expression of IFN-β and ISGs (Fig. 2h). Since YAP/TAZ dKO cells grow extremely slowly and were not practical for use in experiments, we generated $YAP^{low}/TAZ^{-/-}$ NMuMG cells by CRISPR/Cas9 genomic editing and verified the expression of YAP/TAZ (Fig. 2i). $YAP^{low}/TAZ^{-/-}$ NMuMG cells exhibited a significant enhancement of endogenous TBK1 and IRF3 activation following VSV infection (Fig. 2i). These consistent observations suggest that YAP/TAZ negatively regulate cytosolic antiviral sensing and antiviral response.

YAP/TAZ inhibit TBK1 activation independent of transcriptional regulation

To dissect the molecular basis for YAP/TAZ-mediated TBK1 inhibition, we first examined effects of the transcriptionally active

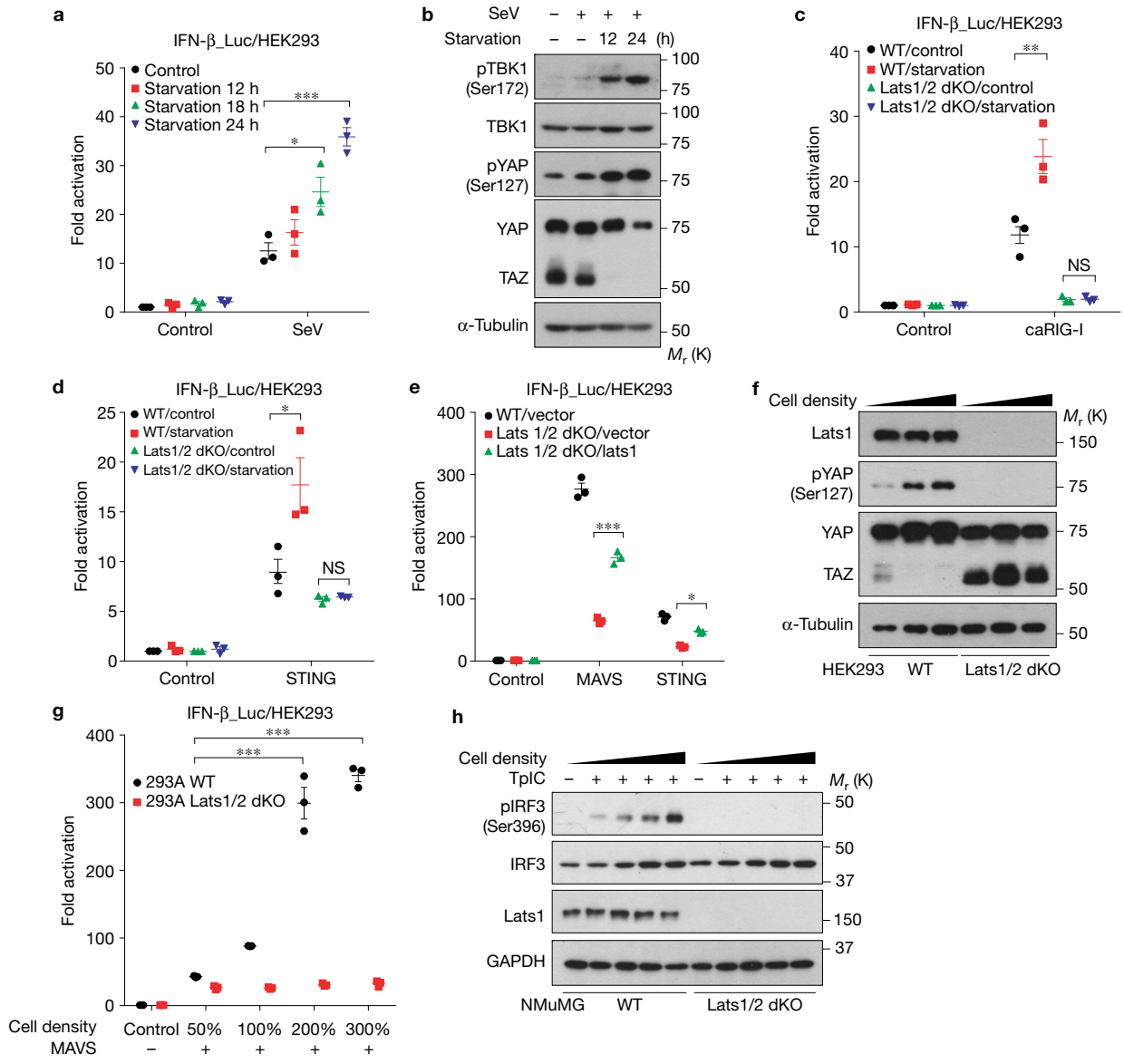

Figure 1 Activation of Hippo signalling enhances cytosolic RNA/DNA sensing. (**a**) Cellular nutrient stress by serum starvation potentiated the IRF3 responsiveness in HEK293T cells stimulated by the infection of Sendai virus (SeV). $n=3$ independent experiments. Mean ± standard error of the mean (s.e.m.). $^{*}P=0.029$, $^{***}P<0.001$, by analysis of variance (ANOVA) test and Bonferroni correction. (**b**) Endogenous TBK1 activation, revealed by immunoblotting TBK1 Ser172 phosphorylation, but not its expression, was profoundly increased following nutrient stress in response to the infection of SeV. As expected, serum starvation activated Hippo signalling, evidenced by enhanced YAP Ser127 phosphorylation and TAZ degradation. (**c**,**d**) Serum starvation boosted IRF3 transactivation in wild-type HEK293A cells, but not in cells with Lats1/2 deletion (dKO), stimulated by the expression of either activated RIG-I (caRIG-I) (**c**) or STING (**d**). IRF3 transactivation was also lower in Lats1/2 dKO cells. $n=3$ independent experiments. Mean ± s.e.m. $^{**}P=0.0038$, $^{*}P=0.022$, by ANOVA test and Bonferroni correction. NS, not significant. (**e**) Reintroduction of Lats1 expression in Lats1/2 dKO cells partially rescued the defect of cytosolic RNA/DNA sensing signalling stimulated by coexpression of MAVS or STING. $n=3$ independent experiments. Mean ± s.e.m. $^{***}P<0.001$, $^{*}P=0.016$, by ANOVA test and Bonferroni correction. (**f**) Strong TAZ accumulation was detected in Lats1/2 dKO HEK293A cells, which failed to respond to cell density for YAP Ser127 phosphorylation and TAZ degradation. (**g**,**h**) Wild-type or Lats1/2 dKO HEK293A or NMuMG cells were transfected with MAVS (**g**) or poly(I:C) (**h**) to activate signalling of cytosolic RNA sensing, and then seeded into different confluence to activate the Hippo pathway. Markedly enhanced IRF3 activation was detected by IFN-β reporter in wild-type cells with high cell density (**g**), or by immunoblotting of endogenous IRF3 Ser396 phosphorylation after poly(I:C) stimulation (**h**). In contrast, Lats1/2 dKO cells failed largely to boost IRF3 activation in response to increased cell density (**g**,**h**). $n=3$ independent experiments. Mean ± s.e.m. $^{***}P<0.001$, by ANOVA test and Bonferroni correction. Unprocessed original scans of blots are shown in Supplementary Fig. 6. Statistics source data are provided in Supplementary Table 1.

(5SA) and inactive (6SA) form of YAP[45–47]. The S94A mutation in the YAP 6SA mutant abolishes its interaction with TEADs and thus is transcriptionally inactive[48,49] (Fig. 3a). Measured by the IFN-β reporter, we unexpectedly observed a profound inhibition of IRF3 transactivation by YAP 6SA, similar to or even stronger than wild-type or active YAP (Fig. 3b). This observation suggests that YAP-mediated suppression might be a direct effect rather than through its transcriptional target(s).

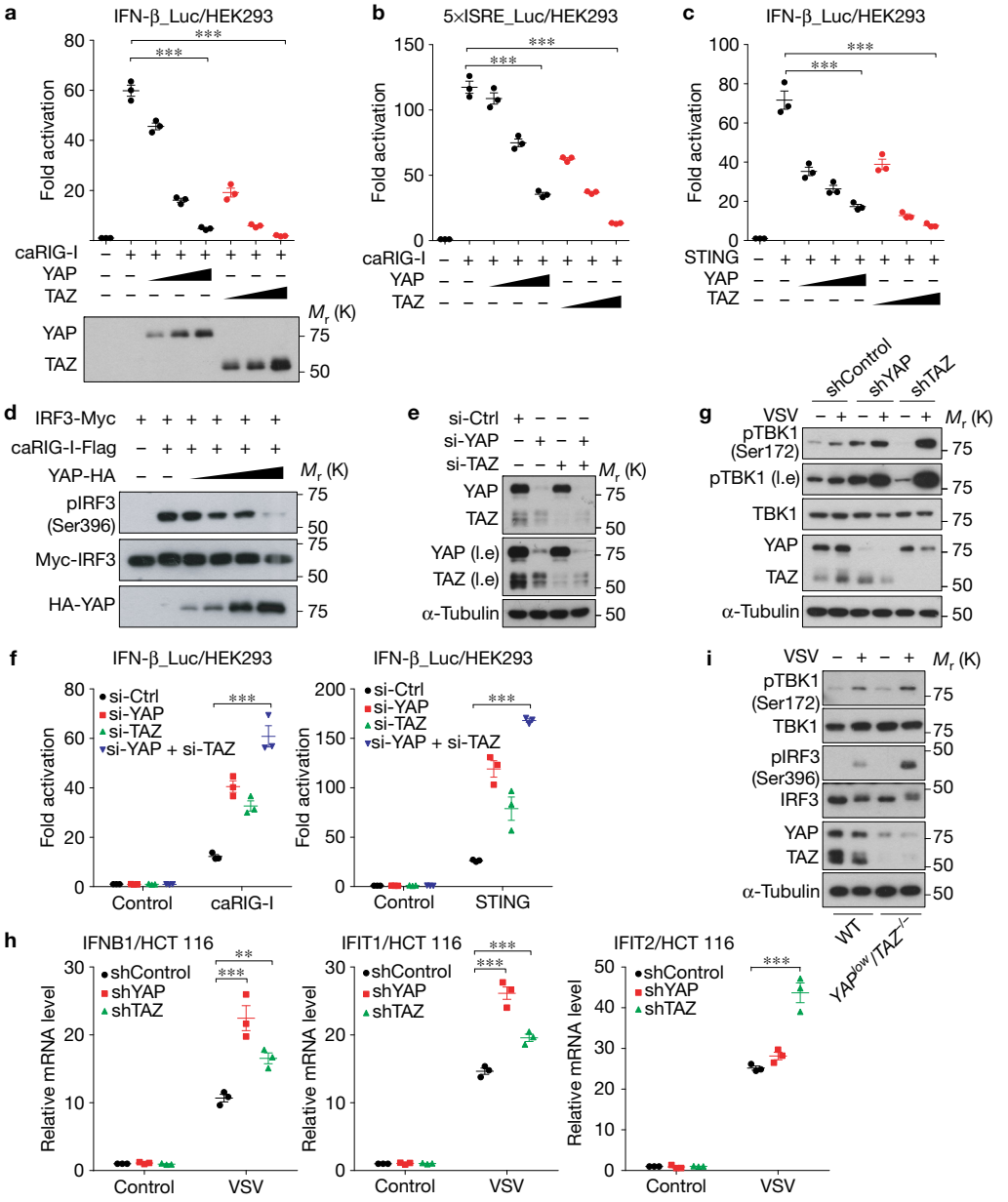

Figure 2 YAP/TAZ attenuate cytosolic RNA/DNA sensing and antiviral responses. (**a**,**b**) Ectopic expression of YAP or TAZ inhibited IRF3 transactivation, which was stimulated by caRIG-I and examined by the IFN-β reporter (**a**) or 5xISRE reporter (**b**), in a dose-dependent manner. $n=3$ independent experiments. Mean ± s.e.m. $^{***}P<0.001$, by ANOVA test and Bonferroni correction. (**c**) STING-induced IRF3 activation, which simulates cytosolic DNA sensing, was suppressed by the co-transfection of YAP or TAZ in a dose-dependent manner. $n=3$ independent experiments. Mean ± s.e.m. $^{***}P<0.001$, by ANOVA test and Bonferroni correction. (**d**) IRF3 activation, stimulated by caRIG-I and detected by immunoblotting of IRF3 phospho-Ser396, was abolished by the coexpression of YAP in a dose-dependent manner. (**e**,**f**) siRNA-mediated knockdown of YAP and/or TAZ in HEK293A cells potentiated the caRIG-I or STING-stimulated IRF3 responsiveness. Higher IRF3 transactivation was detected when both YAP and TAZ were depleted. The efficiency of YAP/TAZ depletion was verified by immunoblotting (**e**). $n=3$ independent experiments. Mean ± s.e.m. $^{***}P<0.001$, by ANOVA test and Bonferroni correction. (**g**) YAP or TAZ in HCT 116 cells was knocked down by shRNA and verified by immunoblotting (fourth panel). VSV infection-induced activation of endogenous TBK1 was more robust after YAP or TAZ depletion. (**h**) VSV infection-induced mRNA expression levels of IFN-β and ISGs were boosted in HCT 116 cells with YAP or TAZ depletion, as evaluated by qRT–PCR assays at 12 hpi. $n=3$ independent experiments. Mean ± s.e.m. $^{***}P<0.001$, $^{**}P=0.0059$ by ANOVA test and Bonferroni correction. (**i**) *YAP*^{low}/*TAZ*$^{-/-}$ NMuMG cells were generated by CRISPR/Cas9-mediated genomic editing and verified by immunoblotting (fifth panel), which exhibited an enhanced level of activation for endogenous TBK1 and IRF3 following VSV infection. Unprocessed original scans of blots are shown in Supplementary Fig. 6. Statistics source data are provided in Supplementary Table 1.

We detected a marked decrease of TBK1 and IKKε activation by co-transfecting of wild-type YAP or YAP 6SA (Fig. 3c,d), or TAZ (Fig. 3e), in a dose-dependent manner. Likewise, YAP 6SA abolished caRIG-I-stimulated IRF3 phosphorylation (Fig. 3f). In an *in vitro* kinase assay with purified TBK1 and using IRF3 as the substrate, we detected a significantly lower catalytic activity of TBK1 when TBK1

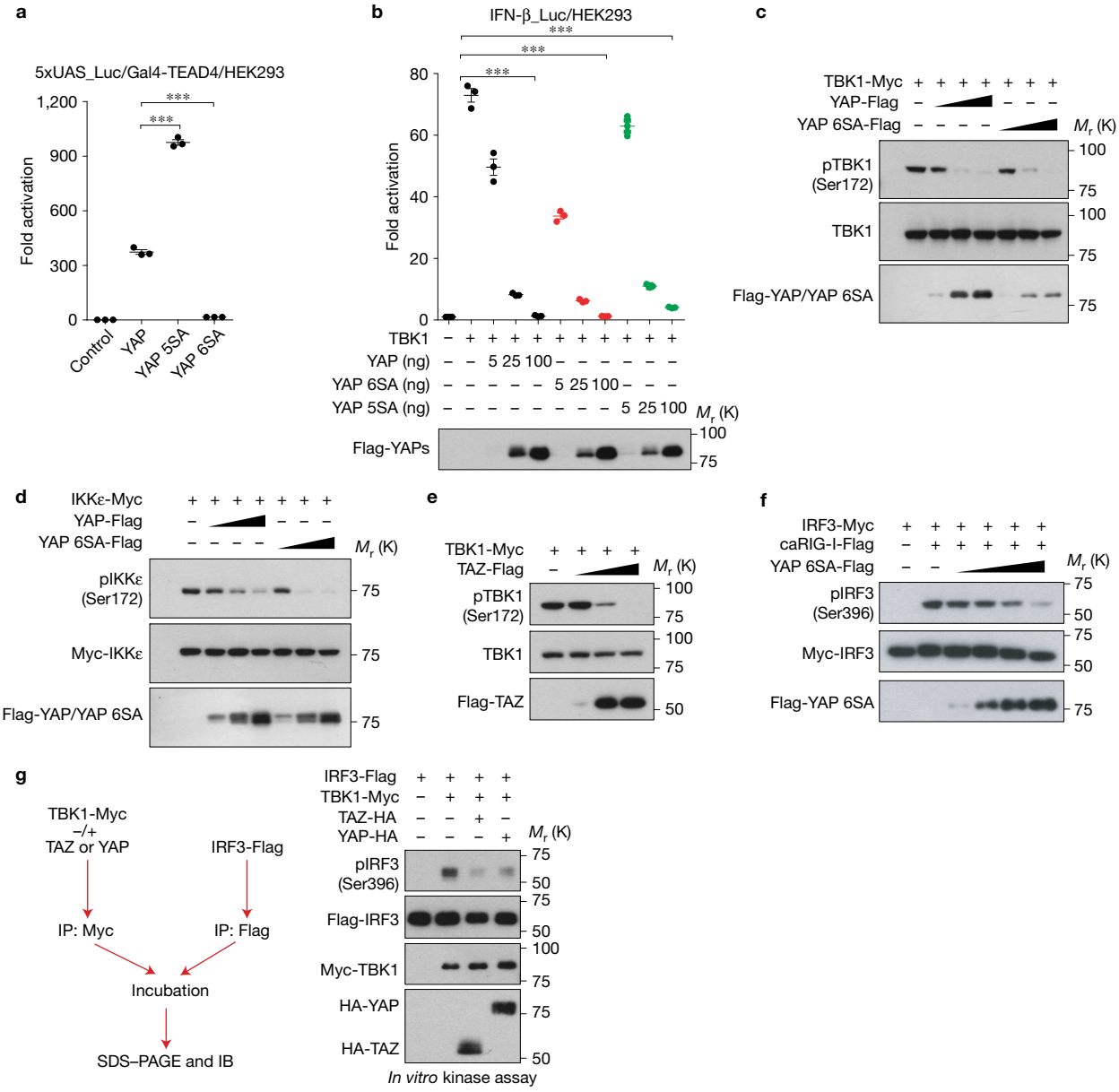

Figure 3 YAP and TAZ abrogate TBK1 activation independent of their transcriptional potential. (**a**,**b**) Ectopic expression of YAP wildtype, the transcriptionally active (5SA) or the transcriptionally inactive (6SA) mutant, elicited similar inhibition on TBK1-induced IRF3 transactivation (**b**, upper panel). Transcriptional potential and expression of YAPs were revealed by TEAD4-responsive reporter (**a**) and by immunoblotting (**b**, lower panel), respectively. $n=3$ independent experiments. Mean ± s.e.m. $^{***}P<0.001$, by ANOVA test and Bonferroni correction. (**c**,**d**) Co-transfection of wild-type or the transcriptionally inactive (6SA) YAP with TBK1/IKKε resulted in the failure of auto-phosphorylation and activation of TBK1 (**c**) or IKKε (**d**), in a dose-dependent manner. (**e**) TAZ expression led to the inactivation of TBK1 in a dose-dependent manner. (**f**) YAP 6SA prevented RIG-I-stimulated activation of IRF3 in a dose-dependent pattern. (**g**) TBK1 isolated from HEK293T cells with YAP or TAZ co-transfection failed to phosphorylate IRF3 *in vitro*, suggesting the loss of TBK1 kinase activity in the presence of YAP or TAZ. Unprocessed original scans of blots are shown in Supplementary Fig. 6. Statistics source data are provided in Supplementary Table 1.

was coexpressed with either YAP or TAZ (Fig. 3g). All of these data suggest that YAP/TAZ inhibit the activation and/or activity of TBK1 in cells.

YAP/TAZ associate with and prevent TBK1 Lys63 ubiquitylation and adaptor/substrate interaction

In elucidating YAP/TAZ-mediated TBK1 inhibition, we detected an endogenous complex of YAP/TAZ and TBK1 in NMuMG cells by co-immunoprecipitation (Fig. 4a), and verified this interaction with transfected proteins (Fig. 4b). We also noticed an obvious mobility shift of YAP in the presence of wild-type TBK1/IKKε (Fig. 4b), suggesting a potential modification of YAP by TBK1/IKKε kinases, although the significance of this regulation was not investigated in this study.

Intriguingly, we found that YAP prevented the association of TBK1/IKKε with their adaptors STING (Fig. 4c,d) and MAVS (Fig. 4e).

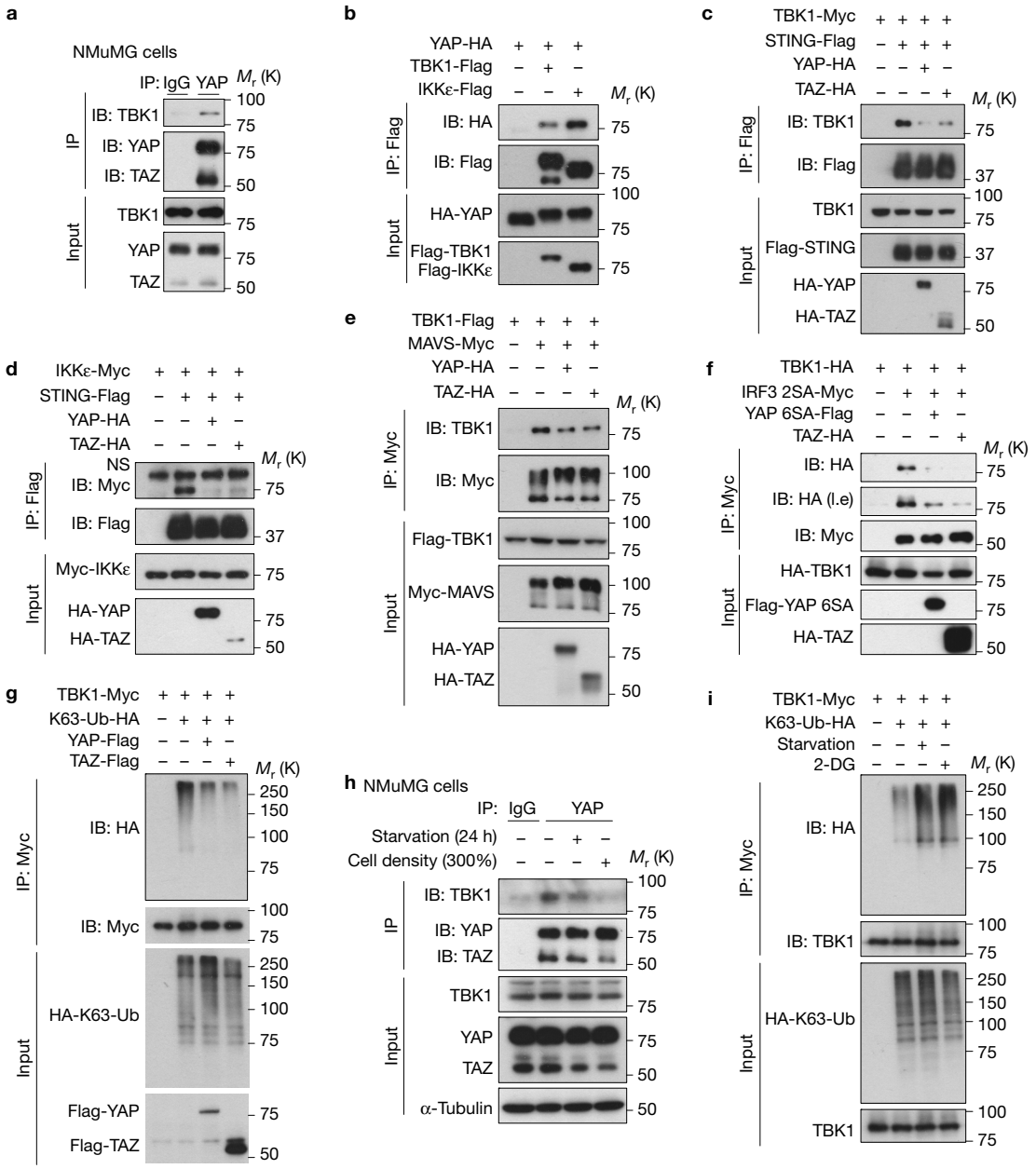

Figure 4 YAP and TAZ associate with and disrupt the TBK1 signalling complex and Lys63 ubiquitylation. (**a**) The endogenous complex of YAP/TAZ and TBK1 in NMuMG cells was detected by co-immunoprecipitation using anti-YAP/TAZ antibody and visualized by using anti-TBK1 antibody. (**b**) Interaction between YAP and TBK1 or IKKε was revealed by co-immunoprecipitation of differentially tagged proteins. (**c**,**d**) Co-transfection of YAP or TAZ impaired STING's recruitment of TBK1 (**c**) and IKKε (**d**), revealed by co-immunoprecipitation. (**e**) Association of MAVS and TBK1 was weakened in the presence of YAP or TAZ, revealed by co-immunoprecipitation. (**f**) Interaction of TBK1 with its substrate IRF3 was severely dampened in the presence of either YAP 6SA or TAZ, as evaluated by co-immunoprecipitation. Note that the IRF3 2SA mutant was used in the experiment to strengthen the interaction between TBK1 and IRF3. (**g**) Lys63-linked ubiquitylation of TBK1, which was detected by coexpression of HA-tagged Lys63-Ub and immunoblotting, was markedly decreased by YAP or TAZ co-transfection. (**h**) The endogenous complex of TBK1 and YAP/TAZ was weakened under serum starvation or high cell density, revealed by co-immunoprecipitation similar to **a**. (**i**) TBK1 Lys63-linked ubiquitylation was strongly enhanced under nutrient or energy stress that activated Hippo signalling. Unprocessed original scans of blots are shown in Supplementary Fig. 6.

Interaction between TBK1 and its substrate IRF3 was also severely compromised in the presence of YAP/TAZ (Fig. 4f). TAZ and the transcriptionally inactive YAP 6SA similarly disrupted TBK1/IKKε interaction with STING, MAVS or IRF3 (Fig. 4c–f). These observations strongly suggest that YAP/TAZ prevent TBK1/IKKε kinases from forming a signalling complex with adaptors and substrates.

TRAFs-mediated TBK1 Lys63-linked ubiquitylation is critical for TBK1 activation[50]. We observed that coexpression of YAP or TAZ reduced TBK1 Lys63 ubiquitylation (Fig. 4g). Consistent with the enhanced antiviral response, a weaker endogenous complex between TBK1 and YAP/TAZ was observed under nutrient or cell–cell contact stresses (Fig. 4h), as well as a more robust TBK1 Lys63

ubiquitylation (Fig. 4i). 2-DG treatment also led to a stronger TBK1 Lys63 ubiquitylation (Fig. 4i), although the effect of 2-DG might be complicated as it suppresses glycolysis and alters inflammatory response[51]. These observations suggest that YAP/TAZ impair TBK1 Lys63 ubiquitylation and the TBK1 signalling complex.

YAP directly inhibits TBK1 activity through the transactivation domain

To dissect the domain(s) of YAP/TAZ required for TBK1 suppression, we generated serial YAP truncations and confirmed their expressions (Fig. 5a). Revealed by the IFN-β reporter assay, we found that the carboxy-terminal transactivation domain of YAP (amino acids 291–488) was necessary and sufficient to abolish IRF3 transactivation (Fig. 5b). Similar to the full-length YAP, the transactivation domain of YAP alone was able to interact with TBK1, abrogate TBK1 activation (Fig. 5c,d), and block the interaction between TBK1 and IRF3 (Fig. 5e). These observations suggest that the YAP transactivation domain is responsible for TBK1 inhibition.

Intriguingly, we observed a direct modification of TBK1 on either full-length YAP or its transactivation domain (Supplementary Fig. 3A,B). We also found that the addition of either YAP or TAZ purified from HEK293T cells abrogated most TBK1- or IKKε-mediated IRF3 phosphorylation *in vitro* (Fig. 5f,g). To further verify this observation, we expressed and purified full-length YAP or its transactivation domain from *Escherichia coli*, and found that full-length YAP and its transactivation domain were both sufficient to block TBK1 catalytic activity in the *in vitro* kinase assay (Fig. 5h). These observations suggest that YAP may directly abolish the catalytic activity of TBK1 by its transactivation domain, probably due to interference of the TBK1–substrate interaction.

YAP/TAZ-mediated TBK1 suppression is relieved by Lats1/2 kinases

We unexpectedly observed that endogenous YAP/TAZ proteins that reside in the nucleus in resting cells were significantly more cytoplasmic in response to VSV infection (Fig. 6a), which was verified by the nuclear/cytoplasmic fractionation (Supplementary Fig. 4A), suggesting a dynamic and reciprocal regulation between Hippo signalling and antiviral response. Although the underlying mechanism exporting YAP/TAZ following virus infection is currently unknown, we noticed that coexpression of either MAVS or TBK1 led to a marked redistribution of transfected YAP or YAP 6SA to the cytoplasm (Fig. 6b). The obviously overlapping distribution of TBK1 with YAP or YAP 6SA also suggested their interaction in the cytoplasm (Fig. 6b).

We next assessed the IKKε–YAP interaction by co-immunoprecipitation and found that both Lats1 and Lats2 weakened IKKε–YAP interaction (Fig. 6c). We also observed that Lats1 relieved the suppressing effect of TAZ on TBK1, evaluated by IRF3 transactivation (Fig. 6d). However, individual point mutations of five known Lats1/2-phosphorylated YAP residues into aspartate showed little effect on YAP-mediated TBK1 suppression (Supplementary Fig. 4B) and YAP Ser127 phosphorylation mimetic also interacted with TBK1 (Supplementary Fig. 4C). On the other hand, activation of Hippo signalling by forskolin[52] also boosted IRF3 transactivation (Fig. 6e). These observations suggest that association of YAP/TAZ to the TBK1/IKKε complex and the inhibition effects are regulated.

YAP and TAZ control the host antiviral defence in cells and zebrafish

We subsequently investigated the physiological significance of YAP/TAZ-mediated TBK1 regulation in antiviral immunity. Stable NMuMG cells for Dox-inducible YAP 6SA expression were generated and verified (Fig. 7a,b, right panels). When YAP 6SA was induced, we observed an enhanced replication level of GFP-tagged VSV or the DNA virus HSV-1, shown by microscopy of GFP^+ (virus replicating) cells and by anti-GFP immunoblotting (Fig. 7a,b). Application of the TBK1 inhibitor BX795 alleviated the effect of YAP 6SA induction (Supplementary Fig. 5A), suggesting that the inhibitory effect of YAP 6SA is mostly through TBK1/IKKε. Expression of MAVS activates antiviral defence and endows host cells for viral resistance[10] (Fig. 7c), whereas coexpression of YAP, TAZ or YAP 6SA impaired MAVS-driven viral resistance and restored VSV replication (Fig. 7c). These data demonstrate the biological function of YAP/TAZ in antiviral host defence and the 'unexpected' function of the transcriptionally inactive YAP.

In contrast, shRNA-mediated depletion of YAP or TAZ decreased the active replication of VSV in HCT 116 cells (Fig. 7d,e), and CRISPR/Cas9-mediated knockout/knockdown of TAZ/YAP in NMuMG cells similarly led to a marked enhancement of antiviral defence, revealed by microscopy or fluorescence-activated cell sorting (FACS) analysis of VSV replication (Fig. 7f,g). Replication of the DNA virus HSV-1 was similarly suppressed in $YAP^{low}/TAZ^{-/-}$ cells (Fig. 7h). Conversely, dKO of Lats1/2 downregulated antiviral signalling (Supplementary Fig. 5B) and boosted VSV replication (Fig. 7i). These observations together suggest a negative biological regulation of YAP/TAZ and a positive regulation of Lats1/2 on cellular antiviral defence.

We then investigated the function of YAP in antiviral defence in whole animals, by using a system previously developed in zebrafish[19,20]. Human YAP 6SA or GFP was ectopically expressed in zebrafish embryos by messenger RNA microinjection at the one-cell stage, followed by gVSV infection at 48 hours post fertilization (hpf). As shown in Fig. 8a and previous reports[19,20], zebrafish embryos underwent a severe VSV infection and started to die around 24–30 hpi. Expression of YAP 6SA sensitized embryos to VSV infection as evidenced by a significant increase in death rate following virus attack (Fig. 8b), as well as suppressed antiviral responses, revealed using quantitative PCR with reverse transcription (qRT–PCR) to assess mRNA expressions of zebrafish IFNs and ISGs (Fig. 8c). These observations suggest a biological and cross-species function of YAP/TAZ in suppression of the antiviral defence in zebrafish.

DISCUSSION

Host antiviral sensing and defence are strictly controlled by intrinsic molecules[53,54]. Still, little is known regarding their regulation by extracellular signals. Here we show that cellular nutrient/density status, through the Hippo–YAP pathway, regulates antiviral host defence (Fig. 8d). Our study reveals that intrinsic activity of the Hippo pathway can integrate and coordinate the outcome of innate host defence. Given that the Hippo pathway mediates signals from cell–cell contact, mechanical stress, matrix stiffness and long-range hormonal signals[55,56], this finding illustrates the possibility for the regulation of innate antiviral immunity by a variety of extracellular cues.

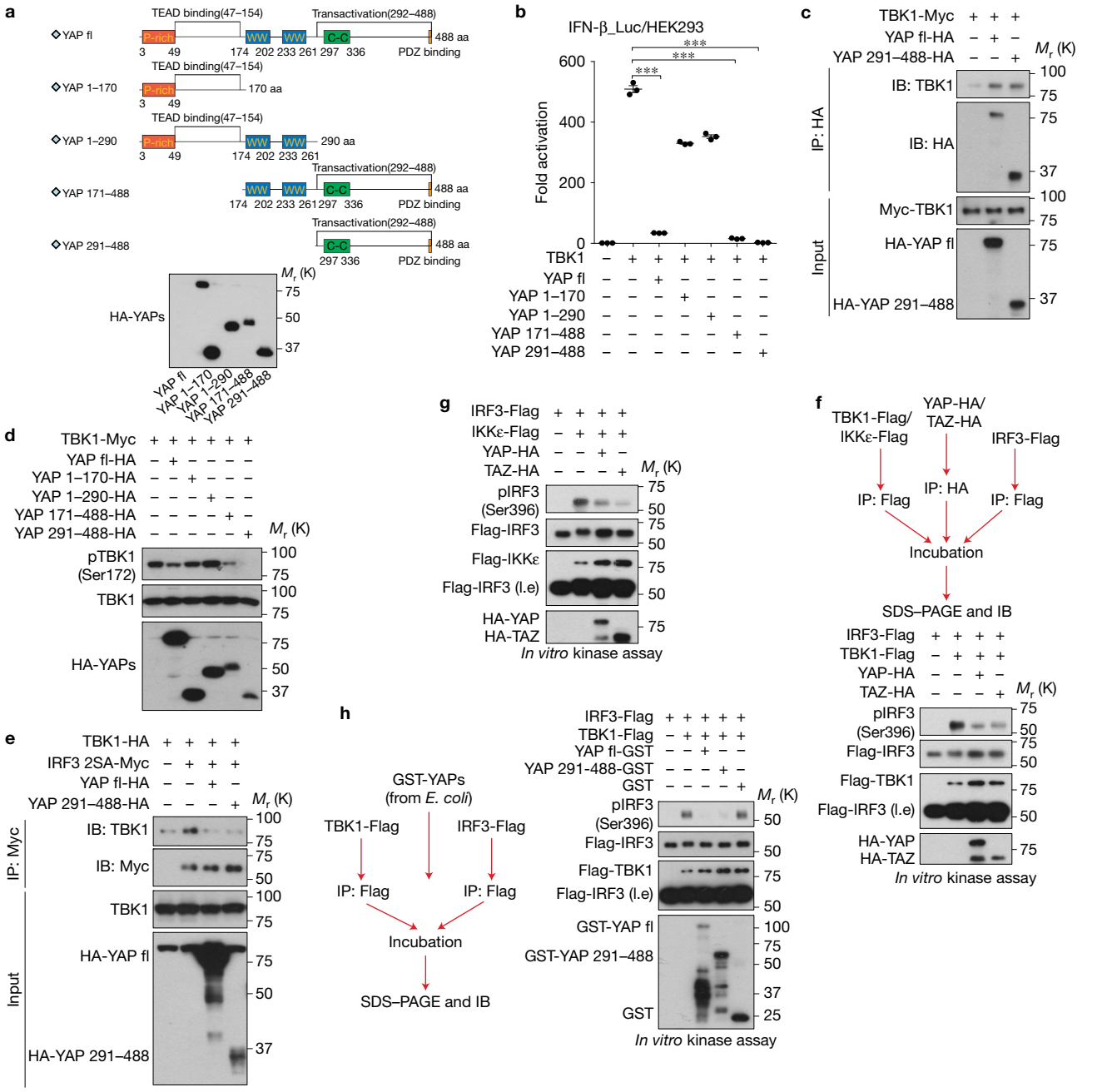

Figure 5 YAP abolishes TBK1 activity through its C-terminal transactivation domain. (**a**,**b**) Serial truncations of YAP were generated as depicted (**a**, upper panel) and their expressions were verified by immunoblotting (**a**, lower panel); effects of the full-length or YAP truncations on antiviral signalling were measured by IRF3 transactivation, which revealed a marked inhibition by YAP transactivation domain (amino acids (aa) 291–488) (**b**). $n=3$ independent experiments. Mean ± s.e.m. $^{***}P<0.001$, by ANOVA test and Bonferroni correction. (**c**,**d**) Similar to the full-length protein, the YAP transactivation domain was sufficient to interact with TBK1 (**c**) and to block TBK1 activation (**d**), assessed by co-immunoprecipitation and by immunoblotting of TBK1 Ser172 phosphorylation, respectively. (**e**) Interaction of TBK1 and IRF3 was severely interrupted in the presence of the YAP transactivation domain, revealed by co-immunoprecipitation. (**f**,**g**) Addition of either YAP or TAZ separately purified from HEK293T cells in the *in vitro* kinase assays suppressed the catalytic activity of TBK1 (**f**) or IKKε (**g**) on the substrate IRF3. (**h**) Likewise, addition of GST-tagged full-length or transactivation domain of YAP that was expressed and purified from *E. coli* blocked TBK1-mediated IRF3 phosphorylation, in an *in vitro* kinase assay. Unprocessed original scans of blots are shown in Supplementary Fig. 6. Statistics source data are provided in Supplementary Table 1.

The observation that YAP/TAZ-mediated TBK1 regulation controls a magnitude of host cells for sensing dangerous signals, such as heterogeneous RNA or DNA, adds a further dimension for the function of the Hippo pathway. This additional layer of regulation could be an adaptive host mechanism to ensure the removal of pathogenic factors but add protection to avoid excessive responses that jeopardize cell survival[57], or to evade potential autoimmune damage from the exposure of self nucleic acids in the cytosol[21,22].

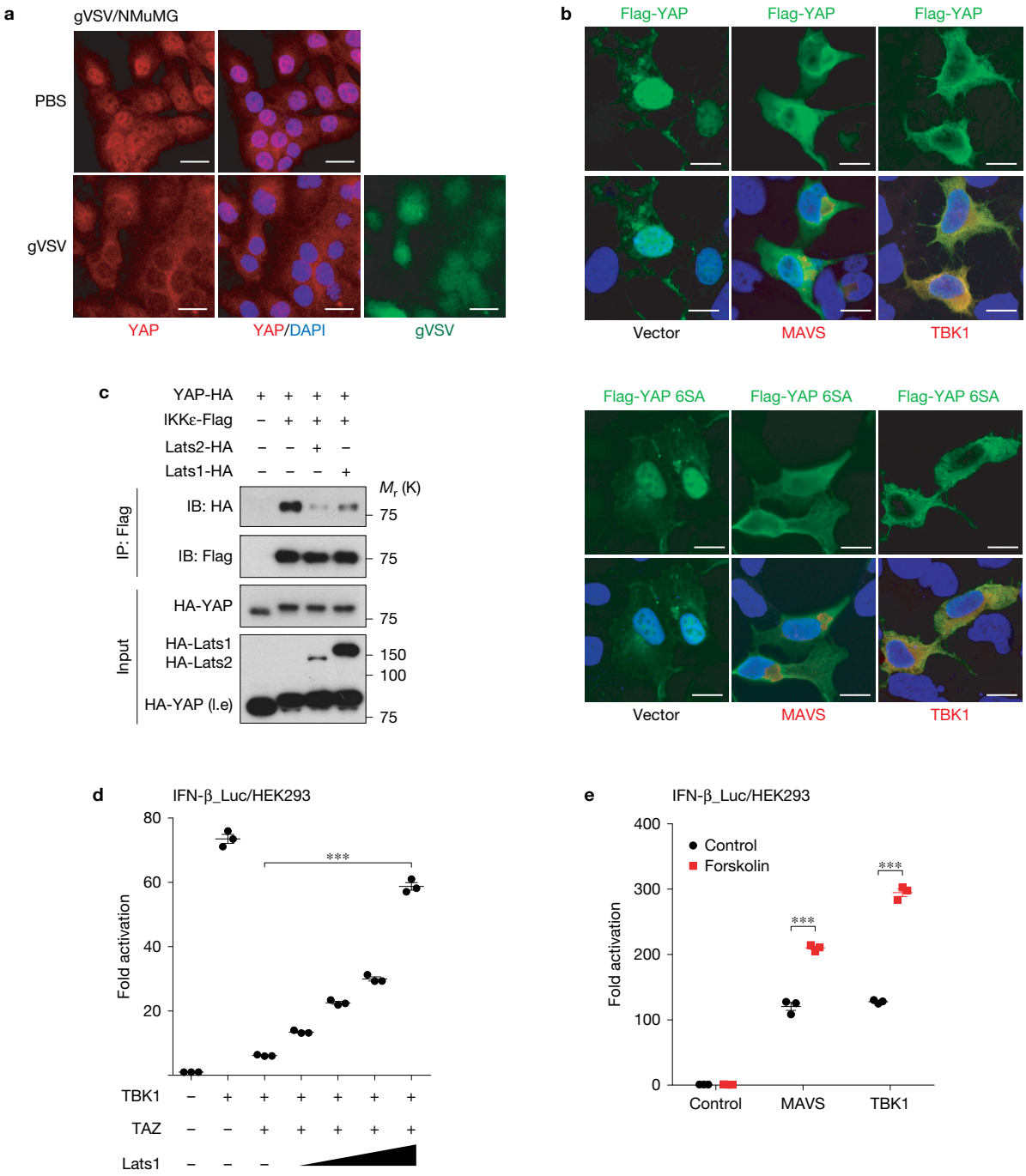

Figure 6 Lats1/2 relieve the association and inhibition of TBK1 by YAP/TAZ. (**a**) Immunofluorescence assay revealed that endogenous YAP/TAZ, which resided richly in the nucleus, was partially exported to the cytoplasm in response to VSV infection. Scale bars, 20 μm. (**b**) YAP wild-type or 6SA mutant, which resided mostly in the nucleus, was exported into the cytoplasm when coexpressed with MAVS or TBK1, revealed by immunofluorescence. The overlap of YAPs and TBK1 in the cytoplasm was evident under confocal microscopy. Scale bars, 10 μm. (**c**) The YAP–IKKε complex was dissociated in the presence of Lats1/2, assessed by co-immunoprecipitation. (**d**) Expression of Lats1 relieved TAZ-mediated suppression of TBK1 in a dose-dependent manner, revealed by IRF3 responsiveness. $n=3$ independent experiments. Mean ± s.e.m. $^{***}P<0.001$, by ANOVA test and Bonferroni correction. (**e**) IRF3 responsiveness, which was stimulated by MAVS or TBK1 coexpression, was boosted in the presence of forskolin, which is known to activate the Hippo pathway. $n=3$ independent experiments. Mean ± s.e.m. $^{***}P<0.001$, by ANOVA test and Bonferroni correction. Unprocessed original scans of blots are shown in Supplementary Fig. 6. Statistics source data are provided in Supplementary Table 1.

Although how YAP/TAZ are regulated by particular conditions, such as GPCR regulation, energy stress and serum starvation, has been well defined[43–46,54,55], their regulation by intracellular conditions or extracellular cues is still not fully understood. Considering the general role of YAP/TAZ in promoting cell proliferation and inhibiting apoptosis[58,59], it is not surprising that YAP/TAZ also

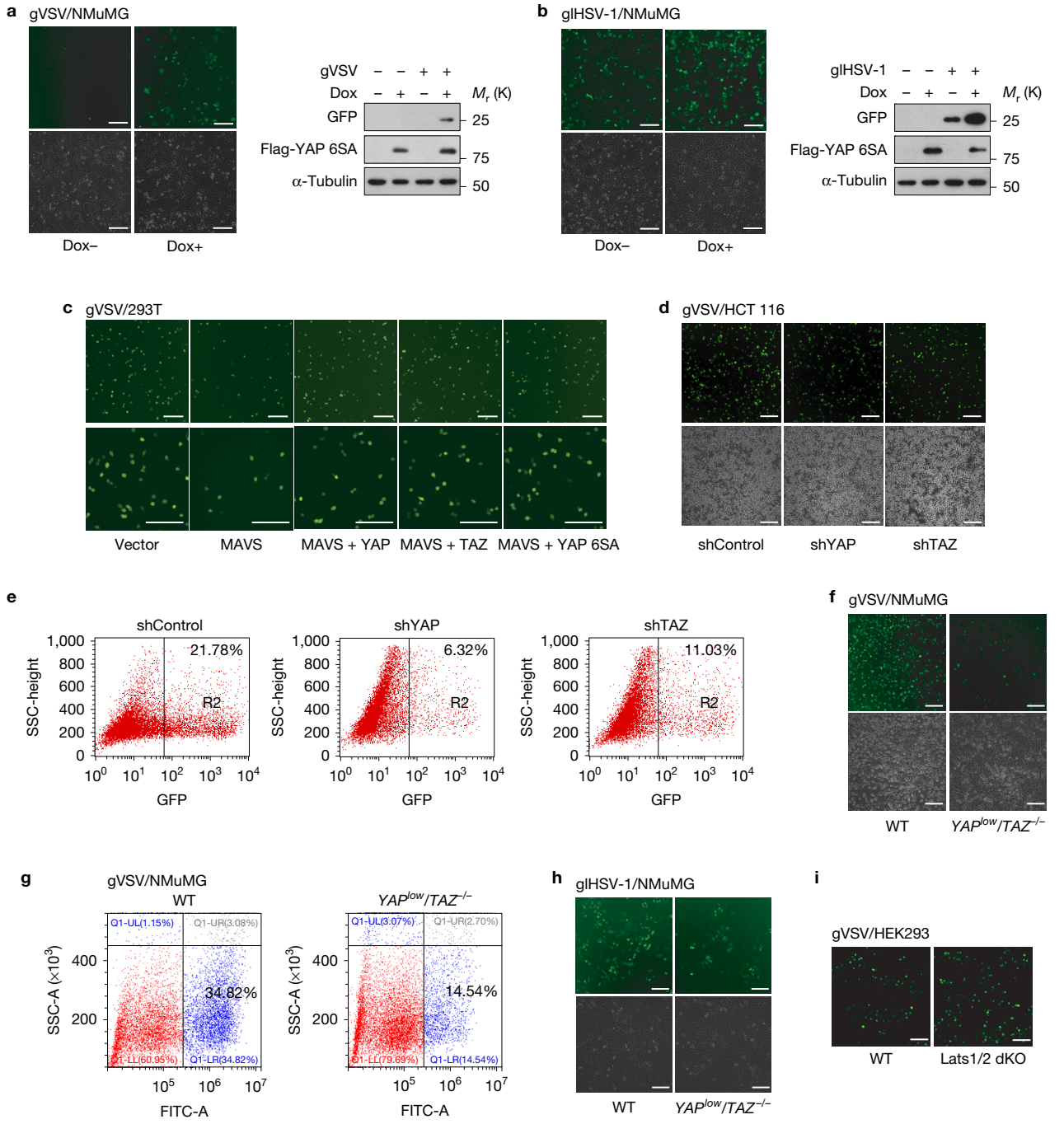

Figure 7 YAP/TAZ control host antiviral defence in cells. (**a**,**b**) Dox-inducible expression of YAP 6SA in NMuMG cells was verified by immunoblotting (right panels). Cellular resistance to GFP-tagged RNA virus VSV (**a**) or DNA virus HSV-1 (**b**) was assessed by microscopy of viral replication (GFP$^+$) cells (left panels) or by GFP immunoblotting (right panels); both revealed an impaired cellular viral resistance under YAP 6SA induction. Scale bars, 100 μm. (**c**) HEK293T cells transfected with MAVS were infected by gVSV, in the absence or presence of YAP wildtype, 6SA or TAZ. The restored number of virus-replication (GFP$^+$) cells indicated that YAPs or TAZ impeded the antiviral function of MAVS. Scale bars, 100 μm. (**d**,**e**) HCT 116 cells with shRNA-mediated YAP or TAZ knockdown exhibited a reduced level of virus replication (GFP$^+$), revealed by microscopy (**d**) or FACS analysis (**e**). Scale bars, 100 μm. (**f**,**g**) Boosted antiviral resistance to gVSV was revealed in *YAP^{low}/TAZ$^{-/-}$* NMuMG cells, evidenced by microscopy (**f**) or FACS analysis (**g**). Scale bars, 100 μm. (**h**) Enhanced cellular resistance to HSV-1 infection was observed in *YAP^{low}/TAZ$^{-/-}$* NMuMG cells, determined by microscopy of virus-replication (GFP$^+$) cells. Scale bars, 100 μm. (**i**) Impaired viral resistance to gVSV infection was observed in Lats1/2 dKO cells by microscopy. Scale bars, 100 μm. Unprocessed original scans of blots are shown in Supplementary Fig. 6.

control cytosolic nucleic acid sensing, which often leads to cell death[60,61]. We believe the direct inhibition of TBK1/IKKε by YAP/TAZ provides a mechanism to neglect the danger signal and to ensure cell survival and proliferation when favourable growth conditions are available. This inhibition may also contribute to regulation of apoptosis and the tumorigenic role of TBK1/IKKε[27,62,63], which

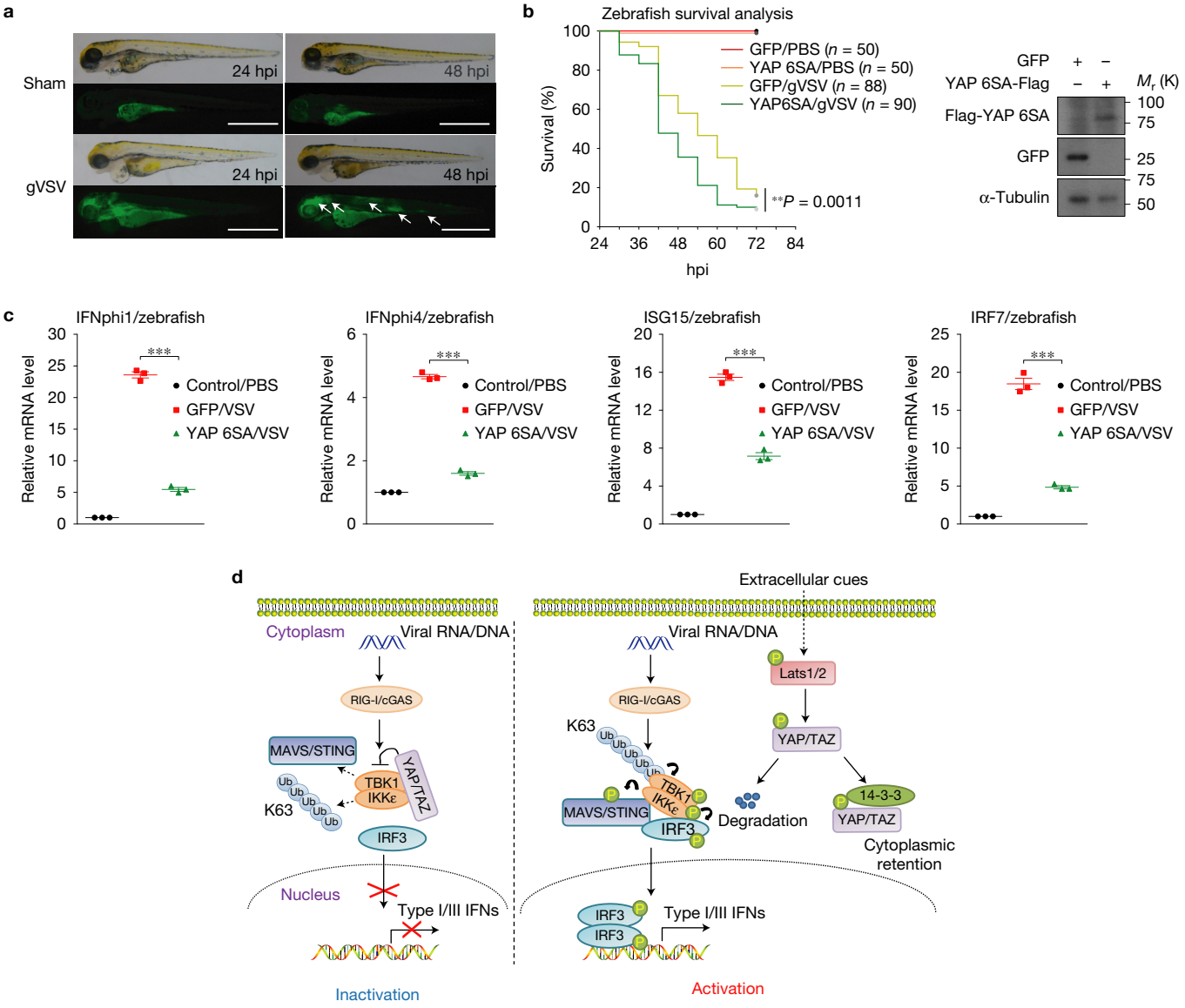

Figure 8 YAP attenuates cytosolic nucleic acid sensing and antiviral defence in zebrafish. (**a**) gVSV was microinjected into the yolk of zebrafish embryos (48 hpf) to elicit a robust virus infection state, which occurred mainly in brain, muscle and gut tissues of fishes, and eventually led to embryonic death at 24–30 hpi. Scale bars, 1 mm. (**b**,**c**) Zebrafish embryos were microinjected at the one-cell stage with *in vitro*-transcribed mRNA to gain expression of GFP or YAP 6SA, verified by immunoblotting (**b**, right panel). A vulnerable phenotype of YAP 6SA-expressing embryos was observed following VSV challenge (**b**, left panel). $n=278$ zebrafish. $^{**}P=0.0011$, by log rank test. In parallel experiments (**c**), zebrafish embryos at 24 hpi were subjected to qRT–PCR analysis to determine the expression of zebrafish IFNs and ISGs mRNA, which revealed a phenotype of suppressed antiviral responses in zebrafish expressing YAP 6SA. $n=3$ independent experiments using 25 embryos for each group. Mean ± s.e.m. $^{***}P<0.001$ by ANOVA test and Bonferroni correction. (**d**) Model for the Hippo–YAP regulation of cytosolic nucleic acid sensing and antiviral defence. YAP/TAZ associate with TBK1/IKKε kinases to prevent their Lys63 ubiquitylation and adaptor/substrate association, thus restricting TBK1/IKKε activation in response to cytosolic nucleic acid sensing. Activation of Hippo signalling through extracellular clues, such as nutrient stress or cell–cell contact, activates Lats1/2 kinases that lead to YAP/TAZ phosphorylation and degradation, thereby relieving their association and inhibition of TBK1/IKKε. Unprocessed original scans of blots are shown in Supplementary Fig. 6. Statistics source data are provided in Supplementary Table 1.

awaits further investigation. TBK1 is involved in maturation of autophagy and bacteria defence[25,64], but little is known regarding whether autophagy, which is also triggered by serum starvation, regulates TBK1 activation. The dependence of Lats1/2 and YAP/TAZ reveals that Hippo signalling, rather than autophagy, is important to mediate antiviral regulation by nutrient/physical stresses. Our current data illustrate the essential focus of Hippo signalling and YAP/TAZ in cytosolic RNA/DNA sensing, which is also well supported by physiological data obtained from cell culture and zebrafish. The fact that cells and zebrafish expressing YAP 6SA are sensitized to RNA/DNA virus infection provides us direct evidence for the physiological involvement of YAP/TAZ in antiviral defence, independent of their transcriptional activity. Since the host defence imbalance is a main cause of autoimmune diseases[21,22], it is worthy

to examine whether YAP/TAZ and the Hippo pathway are involved in these situations.

Pathogenic nucleic acids are sensed in the cytosol by RIG-I-like receptors and/or cGAS[1,6]. TBK1 is central for this cytosolic RNA/DNA sensing, acting as a downstream signal mediator of mitochondria-conjugated MAVS or ER-associated STING to transduce the recognition signal to the transcriptional factors IRF3/IRF7, to induce the expression of antiviral cytokines and a variety of ISGs[54]. MAVS self-associates and polymerizes on mitochondria to set the platform for functional signal complexes[14], while STING-mediated TBK1 activation is thought to be executed in the microsome[65,66]. Our data of YAP/TAZ re-localization during virus infection and their formation of endogenous complex with TBK1 suggest that YAP/TAZ are regulatory components for these antiviral signalling complexes. The presence of YAP/TAZ prevents the Lys63 ubiquitylation of TBK1, which is critical for TBK1 activation[15,50,67,68]. We did not dissect the possible causation for this regulation, but noticed that the interaction between TBK1 and adaptors MAVS or STING, or with the substrate IRF3, is disrupted by YAP/TAZ. Our data also showed that YAP/TAZ inhibit TBK1 kinase activity *in vitro*, probably through direct association with TBK1 to cover its catalytic centre or to compete with IRF3 as a substrate.

Conversely, nutrient starvation or cell–cell contact activates Lats1/2, which removes the inhibition of YAP/TAZ on TBK1 and sensitizes host cells for danger signals. Distinct from our previous finding of Mst1 in antiviral immunity that is independent of Lats1/2 and Hippo signalling[20], the regulation by cellular nutrient/physical stress requires Lats1/2 kinase. Intriguingly, YAP with the Ser94 to alanine mutation, which disrupts YAP–TEAD complex formation[49], retains the same inhibitory effect. Purified full-length or transactivation domain of YAP also directly blocks the kinase activities of TBK1/IKKε, suggesting an alternative function mode of YAP/TAZ by direct protein–protein interaction, rather than through its transcriptional co-activators potential. We noticed that Lats1/2 can effectively dissociate YAP from TBK1/IKKε and relieve TBK1 inhibition, indicating that YAP/TAZ-mediated TBK1 inhibition is controlled, although the exact mechanism requires further investigation.

In conclusion, our study provides an unusual function and signal integration of the Hippo pathway to TBK1 activation through an unexpected mechanism. Our model indicates that the level and activity of the Hippo components can serve as a determinant to regulate the magnitude of host antiviral responses. Consistent with this notion, our research suggests that pharmacological manipulation of these signal mediators may offer potential therapeutic benefits for antiviral prevention. □

METHODS

Methods, including statements of data availability and any associated accession codes and references, are available in the online version of this paper.

Note: Supplementary Information is available in the online version of the paper

ACKNOWLEDGEMENTS

We are grateful to Z. J. Chen (UT Southwestern Medical Center, Dallas, USA), for gVSV virus, J. Han (Xiamen University, Xiamen, China) for glHSV-1 virus, and Z. Xia, Y. Huang, X. Wang and J. Jin (all Zhejiang University, China) for reagents. This research was partly supported by MoST 973 Plan (2015CB553800), NSFC Project (81472665, 91540205 and 31571447), CPSF (581220-X91602), DoD grant (1W81XWH-15-1-0650), NIH (R01GM051586, R35CA196878, and R21CA209007), and Project 985 and the Fundamental Research Funds for the Central Universities to the Life Sciences Institute at Zhejiang University. P.X. is a scholar in the National 1000 Young Talents Program.

AUTHOR CONTRIBUTIONS

Q.Z. and F.M. carried out most experiments. S.C., S.W., S.L., R.Z., J.W. and J.Q. contributed to several experiments, S.W.P., X.L., B.Z., J.L., J.Z., X.-H.F. and K.-L.G. helped with data analyses and discussions. P.X. conceived the study and experimental design and wrote the manuscript.

COMPETING FINANCIAL INTERESTS

K.-L.G. co-founded but receives no direct financial support from Vivace Therapeutics. All other authors declare no competing financial interests.

Published online at http://dx.doi.org/10.1038/ncb3496

1. Yoneyama, M. *et al.* The RNA helicase RIG-I has an essential function in double-stranded RNA-induced innate antiviral responses. *Nat. Immunol.* **5,** 730–737 (2004).
2. Hornung, V. *et al.* 5′-Triphosphate RNA is the ligand for RIG-I. *Science* **314,** 994–997 (2006).
3. Li, X. D. *et al.* Pivotal roles of cGAS-cGAMP signaling in antiviral defense and immune adjuvant effects. *Science* **341,** 1390–1394 (2013).
4. Civril, F. *et al.* Structural mechanism of cytosolic DNA sensing by cGAS. *Nature* **498,** 332–337 (2013).
5. Gao, P. *et al.* Cyclic [G(2′,5′)pA(3′,5′)p] is the metazoan second messenger produced by DNA-activated cyclic GMP-AMP synthase. *Cell* **153,** 1094–1107 (2013).
6. Sun, L., Wu, J., Du, F., Chen, X. & Chen, Z. J. Cyclic GMP-AMP synthase is a cytosolic DNA sensor that activates the type I interferon pathway. *Science* **339,** 786–791 (2013).
7. Orzalli, M. H. & Knipe, D. M. Cellular sensing of viral DNA and viral evasion mechanisms. *Annu. Rev. Microbiol.* **68,** 477–492 (2014).
8. Fitzgerald, K. A. *et al.* IKKε and TBK1 are essential components of the IRF3 signaling pathway. *Nat. Immunol.* **4,** 491–496 (2003).
9. Sharma, S. *et al.* Triggering the interferon antiviral response through an IKK-related pathway. *Science* **300,** 1148–1151 (2003).
10. Seth, R. B., Sun, L., Ea, C. K. & Chen, Z. J. Identification and characterization of MAVS, a mitochondrial antiviral signaling protein that activates NF-κB and IRF 3. *Cell* **122,** 669–682 (2005).
11. Ishikawa, H. & Barber, G. N. STING is an endoplasmic reticulum adaptor that facilitates innate immune signalling. *Nature* **455,** 674–678 (2008).
12. Chan, Y. K. & Gack, M. U. RIG-I-like receptor regulation in virus infection and immunity. *Curr. Opin. Virol.* **12,** 7–14 (2015).
13. Akira, S., Uematsu, S. & Takeuchi, O. Pathogen recognition and innate immunity. *Cell* **124,** 783–801 (2006).
14. Hou, F. *et al.* MAVS forms functional prion-like aggregates to activate and propagate antiviral innate immune response. *Cell* **146,** 448–461 (2011).
15. Tu, D. *et al.* Structure and ubiquitination-dependent activation of TANK-binding kinase 1. *Cell Rep.* **3,** 747–758 (2013).
16. tenOever, B. R. *et al.* Activation of TBK1 and IKKε kinases by vesicular stomatitis virus infection and the role of viral ribonucleoprotein in the development of interferon antiviral immunity. *J. Virol.* **78,** 10636–10649 (2004).
17. Tojima, Y. *et al.* NAK is an IκB kinase-activating kinase. *Nature* **404,** 778–782 (2000).
18. Solis, M. *et al.* Involvement of TBK1 and IKKε in lipopolysaccharide-induced activation of the interferon response in primary human macrophages. *Eur. J. Immunol.* **37,** 528–539 (2007).
19. Xiang, W. *et al.* PPM1A silences cytosolic RNA sensing and antiviral defense through direct dephosphorylation of MAVS and TBK1. *Sci. Adv.* **2,** e1501889 (2016).
20. Meng, F. *et al.* Mst1 shuts off cytosolic antiviral defense through IRF3 phosphorylation. *Genes Dev.* **30,** 1086–1100 (2016).
21. Gao, D. *et al.* Activation of cyclic GMP-AMP synthase by self-DNA causes autoimmune diseases. *Proc. Natl Acad. Sci. USA* **112,** E5699–E5705 (2015).
22. Crampton, S. P. & Bolland, S. Spontaneous activation of RNA-sensing pathways in autoimmune disease. *Curr. Opin. Immunol.* **25,** 712–719 (2013).
23. Pomerantz, J. L. & Baltimore, D. NF-κB activation by a signaling complex containing TRAF2, TANK and TBK1, a novel IKK-related kinase. *EMBO J.* **18,** 6694–6704 (1999).
24. Baldwin, A. S. Regulation of cell death and autophagy by IKK and NF-κB: critical mechanisms in immune function and cancer. *Immunol. Rev.* **246,** 327–345 (2012).
25. Pilli, M. *et al.* TBK-1 promotes autophagy-mediated antimicrobial defense by controlling autophagosome maturation. *Immunity* **37,** 223–234 (2012).
26. Ou, Y. H. *et al.* TBK1 directly engages Akt/PKB survival signaling to support oncogenic transformation. *Mol. Cell* **41,** 458–470 (2011).

27. Barbie, D. A. *et al.* Systematic RNA interference reveals that oncogenic KRAS-driven cancers require TBK1. *Nature* **462,** 108–112 (2009).
28. Harvey, K. F., Pfleger, C. M. & Hariharan, I. K. The *Drosophila* Mst ortholog, hippo, restricts growth and cell proliferation and promotes apoptosis. *Cell* **114,** 457–467 (2003).
29. Wu, S., Huang, J., Dong, J. & Pan, D. Hippo encodes a Ste-20 family protein kinase that restricts cell proliferation and promotes apoptosis in conjunction with salvador and warts. *Cell* **114,** 445–456 (2003).
30. Pantalacci, S., Tapon, N. & Leopold, P. The Salvador partner Hippo promotes apoptosis and cell-cycle exit in *Drosophila*. *Nat. Cell Biol.* **5,** 921–927 (2003).
31. Udan, R. S., Kango-Singh, M., Nolo, R., Tao, C. & Halder, G. Hippo promotes proliferation arrest and apoptosis in the Salvador/Warts pathway. *Nat. Cell Biol.* **5,** 914–920 (2003).
32. Pan, D. The hippo signaling pathway in development and cancer. *Dev. Cell* **19,** 491–505 (2010).
33. Zhao, B., Li, L., Lei, Q. & Guan, K. L. The Hippo-YAP pathway in organ size control and tumorigenesis: an updated version. *Genes Dev.* **24,** 862–874 (2010).
34. Zhao, B. *et al.* TEAD mediates YAP-dependent gene induction and growth control. *Genes Dev.* **22,** 1962–1971 (2008).
35. Varelas, X. *et al.* The Hippo pathway regulates Wnt/β-catenin signaling. *Dev. Cell* **18,** 579–591 (2010).
36. Mo, J. S., Yu, F. X., Gong, R., Brown, J. H. & Guan, K. L. Regulation of the Hippo-YAP pathway by protease-activated receptors (PARs). *Genes Dev.* **26,** 2138–2143 (2012).
37. Yu, F. X. *et al.* Regulation of the Hippo-YAP pathway by G-protein-coupled receptor signaling. *Cell* **150,** 780–791 (2012).
38. Miller, E. *et al.* Identification of serum-derived sphingosine-1-phosphate as a small molecule regulator of YAP. *Chem. Biol.* **19,** 955–962 (2012).
39. Bao, Y. *et al.* A cell-based assay to screen stimulators of the Hippo pathway reveals the inhibitory effect of dobutamine on the YAP-dependent gene transcription. *J. Biochem.* **150,** 199–208 (2011).
40. Varelas, X. *et al.* TAZ controls Smad nucleocytoplasmic shuttling and regulates human embryonic stem-cell self-renewal. *Nat. Cell Biol.* **10,** 837–848 (2008).
41. Camargo, F. D. *et al.* YAP1 increases organ size and expands undifferentiated progenitor cells. *Curr. Biol.* **17,** 2054–2060 (2007).
42. Liu, B. *et al.* Toll receptor-mediated hippo signaling controls innate immunity in *Drosophila*. *Cell* **164,** 406–419 (2016).
43. Zhao, B., Tumaneng, K. & Guan, K. L. The Hippo pathway in organ size control, tissue regeneration and stem cell self-renewal. *Nat. Cell Biol.* **13,** 877–883 (2011).
44. Thaventhiran, J. E. *et al.* Activation of the Hippo pathway by CTLA-4 regulates the expression of Blimp-1 in the $CD8^{+}$T cell. *Proc. Natl Acad. Sci. USA* **109,** E2223–E2229 (2012).
45. Zhao, B. *et al.* Inactivation of YAP oncoprotein by the Hippo pathway is involved in cell contact inhibition and tissue growth control. *Genes Dev.* **21,** 2747–2761 (2007).
46. Mo, J. S. *et al.* Cellular energy stress induces AMPK-mediated regulation of YAP and the Hippo pathway. *Nat. Cell Biol.* **17,** 500–510 (2015).
47. Wang, W. *et al.* AMPK modulates Hippo pathway activity to regulate energy homeostasis. *Nat. Cell Biol.* **17,** 490–499 (2015).
48. Chen, L. *et al.* Structural basis of YAP recognition by TEAD4 in the hippo pathway. *Genes Dev.* **24,** 290–300 (2010).
49. Li, Z. *et al.* Structural insights into the YAP and TEAD complex. *Genes Dev.* **24,** 235–240 (2010).
50. Li, S., Wang, L., Berman, M., Kong, Y. Y. & Dorf, M. E. Mapping a dynamic innate immunity protein interaction network regulating type I interferon production. *Immunity* **35,** 426–440 (2011).
51. Tannahill, G. M. *et al.* Succinate is an inflammatory signal that induces IL-1β through HIF-1α. *Nature* **496,** 238–242 (2013).
52. Yu, F. X. *et al.* Protein kinase A activates the Hippo pathway to modulate cell proliferation and differentiation. *Genes Dev.* **27,** 1223–1232 (2013).
53. Liu, J., Qian, C. & Cao, X. Post-translational modification control of innate immunity. *Immunity* **45,** 15–30 (2016).
54. Wu, J. & Chen, Z. J. Innate immune sensing and signaling of cytosolic nucleic acids. *Annu. Rev. Immunol.* **32,** 461–488 (2014).
55. Low, B. C. *et al.* YAP/TAZ as mechanosensors and mechanotransducers in regulating organ size and tumor growth. *FEBS Lett.* **588,** 2663–2670 (2014).
56. Meng, Z., Moroishi, T. & Guan, K. L. Mechanisms of Hippo pathway regulation. *Genes Dev.* **30,** 1–17 (2016).
57. Porritt, R. A. & Hertzog, P. J. Dynamic control of type I IFN signalling by an integrated network of negative regulators. *Trends Immunol.* **36,** 150–160 (2015).
58. Yu, F. X., Zhao, B. & Guan, K. L. Hippo pathway in organ size control, tissue homeostasis, and cancer. *Cell* **163,** 811–828 (2015).
59. Huang, J., Wu, S., Barrera, J., Matthews, K. & Pan, D. The Hippo signaling pathway coordinately regulates cell proliferation and apoptosis by inactivating Yorkie, the *Drosophila* homolog of YAP. *Cell* **122,** 421–434 (2005).
60. Barber, G. N. Host defense, viruses and apoptosis. *Cell Death Differ.* **8,** 113–126 (2001).
61. Upton, J. W. & Chan, F. K. Staying alive: cell death in antiviral immunity. *Mol. Cell* **54,** 273–280 (2014).
62. Ou, Y. H. *et al.* TBK1 directly engages Akt/PKB survival signaling to support oncogenic transformation. *Mol. Cell* **41,** 458–470 (2011).
63. Xie, X. *et al.* IκB kinase ϵ and TANK-binding kinase 1 activate AKT by direct phosphorylation. *Proc. Natl Acad. Sci. USA* **108,** 6474–6479 (2011).
64. Wild, P. *et al.* Phosphorylation of the autophagy receptor optineurin restricts Salmonella growth. *Science* **333,** 228–233 (2011).
65. Ishikawa, H., Ma, Z. & Barber, G. N. STING regulates intracellular DNA-mediated, type I interferon-dependent innate immunity. *Nature* **461,** 788–792 (2009).
66. Chen, Q., Sun, L. & Chen, Z. J. Regulation and function of the cGAS-STING pathway of cytosolic DNA sensing. *Nat. Immunol.* **17,** 1142–1149 (2016).
67. Larabi, A. *et al.* Crystal structure and mechanism of activation of TANK-binding kinase 1. *Cell Rep.* **3,** 734–746 (2013).
68. Shu, C. *et al.* Structural insights into the functions of TBK1 in innate antimicrobial immunity. *Structure* **21,** 1137–1148 (2013).

METHODS

Expression plasmids, reagents and antibodies. Expression plasmids encoding Flag-, Myc- or HA-tagged wild-type or mutations of human TBK1, IKKε, IRF3, caRIG-I, MAVS, STING, TAZ, YAP, Lats1, Lats2, TRIF, MyD88, Lys63-Ub, caALK5, and reporters of TCF, Gli1, 4SBE, NF-κB, 5xUAS, IFN-β_Luc and 5xISRE_Luc have been described previously[19,69]. YAP truncations including YAP amino acids 1–170, 1–290, 171–488, 291–488, and the GST-tagged YAP full-length and amino acids 291–488 were generated by PCR-based cloning performed by pfu DNA polymerase from Stratagene. Detailed information will be provided on request. All coding sequences were verified by DNA sequencing.

GFP and luciferase double-tagged HSV-1 was a gift from J. Han (Xiamen University, Xiamen, China), GFP-tagged VSV was a gift from Z. J. Chen (UT Southwestern Medical Center, Dallas, USA), and Sendai virus (Cantell strain) was from Charles River Laboratories. The pharmacological reagents BX795 (Millipore), 2-DG (Sangon Biotech), doxycycline (Sangon Biotech) and poly(I:C) (Invivogen) were purchased.

Detailed information for all antibodies applied in immunoblotting, immunoprecipitation and immunofluorescence is provided in Supplementary Table 2.

Cell culture, transfections and infections. NMuMG, HEK293, HCT 116, HaCaT and THP-1 cells were obtained from ATCC. Peritoneal macrophages were obtained from C57BL/6 male mice at 6–8 weeks of age by the Brewer thioglycollate medium (Sigma)-induced approach, and MEFs were obtained from E12.5–E13.5 embryos in pregnant C57BL/6 female mice at 8 weeks of age, and immortalized by infection of viral vector packaging SV40. Care of experimental animals was in accordance with guidelines and approved by the laboratory animal committee of Zhejiang University. No cell lines used in this study were found in the database of commonly misidentified cell lines that is maintained by ICLAC and NCBI Biosample. Cell lines were frequently checked in morphology under microscopy and tested for mycoplasma contamination, but were not authenticated. All cell lines, except for THP-1 that was maintained in RPMI 1640 medium, were cultured in DMEM medium with 10% fetal bovine serum (FBS) at 37 °C in 5% CO_2 (v/v). The YAP 6SA inducible expressing NMuMG and MEF cells were generated by lentiviral vector containing the inducible Tet-on system followed by the open reading frame (ORF) of the YAP 6SA mutant, and selected by G418 antibiotic at concentration of 1,500 μg ml^{-1} for one week. Xtremegene HP (Roche) or polythylenimine (PEI, Polysciences) transfection reagents were used for plasmid transfection. Transfection of poly(I:C) was performed by using Lipofectamine RNAiMAX (Invitrogen) reagent. Infection of Sendai virus (SeV), vesicular stomatitis virus (VSV), and herpes simplex virus-1 (HSV-1) was as previously described[19,20]. Briefly, viruses with indicated amount (0.5–5 moi) were added into the fresh and serum-free medium, and cells were incubated at 37 °C in 5% CO_2 (v/v) for 1 h, shaking mildly every 15 min. Virus-containing medium was then replaced by fresh medium containing 10% FBS.

Luciferase reporter assay. HEK293T or HEK293A cells were transfected with the indicated reporters (100 ng) bearing an ORF coding Firefly luciferase, along with the pRL-Luc with *Renilla* luciferase coding as the internal control for transfection, and other expression vectors specified in the results section. In brief, cells were cultured for 12 h post transfection, and stimulated by virus infection or transfection with poly(I:C). After 24 h of transfection and with indicated treatment, cells were lysed by passive lysis buffer (Promega). Luciferase assays were performed using a dual luciferase assay kit (Promega), quantified with POLARstar Omega (BMG Labtech), and normalized to the internal *Renilla* luciferase control.

Quantitative RT–PCR assay. The HCT 116 cells or embryos of zebrafish with specified viral infection were lysed and total RNA was extracted using the RNAeasy extraction kit (Invitrogen). cDNA was generated by the one-step iScript cDNA synthesis kit (Vazyme), and quantitative real-time PCR was performed using the EvaGreen Qpcr MasterMix (Abm) and CFX96 real-time PCR system (Bio-Rad). Relative quantification was expressed as $2^{-\Delta}$Ct, where $^{\Delta}$Ct is the difference between the main Ct value of triplicates of the sample and that of an endogenous L19 or GAPDH mRNA control. The human or zebrafish primer sequences used can be found in Supplementary Table 3.

Co-immunoprecipitations and immunoblottings. HEK293T or NMuMG cells infected with VSV/SeV, or transfected for 36 h with specified plasmids encoding amino-terminal Myc-, Flag-, or HA-tagged YAP, TAZ, TBK1, IKKε, IRF3, caRIG-I, MAVS or STING, were lysed using a modified Myc lysis buffer (MLB)[69] (20 mM Tris-Cl, 200 mM NaCl, 10 mM NaF, 1 mM NaV_2O_4, 1% NP-40, 20 mM β-glycerophosphate, and protease inhibitor, pH 7.5). Cell lysates were then subjected to immunoprecipitation using anti-Flag, anti-Myc or anti-HA antibodies for transfected proteins, or using anti-YAP/TAZ antibodies for endogenous proteins. After 3–4 washes with MLB, adsorbed proteins in beads were resolved by 2 × SDS loading buffer and analysed by SDS–PAGE and immunoblotting with indicated antibodies. Cell lysates were also analysed by SDS–PAGE and immunoblotting to control protein abundance. Nuclear and cytoplasmic extracts were prepared using the NE-PER Nuclear and Cytoplasmic Extraction kit (Pierce), according to the manufacturer's instructions. Detailed information of all antibodies used in immunoprecipitation assays is provided in Supplementary Table 2.

siRNA or shRNA-mediated RNA interference. Double-stranded siRNA (RiboBio) to silence endogenous YAP or TAZ expression in HEK293 cells targeted the human YAP or TAZ mRNA (sequence information is in Supplementary Table 3). Control siRNA (RiboBio) was used to control for possible nonspecific effects of RNA interference. Cells were transfected with siRNA using the Lipofectamine RNAiMAX (Invitrogen) reagent for 48 h before the further assay, and the reverse transfection method was used to reach optimal efficiency. The shRNA-mediated knockdown of YAP or TAZ in HCT 116 cells was generated by shRNAs as previously described[34,37], delivered by the lentiviral vector produced by the Mission shRNA (Sigma Aldrich) plasmids (TRCN information is in Supplementary Table 3), together with pMD2.G and psPAX2 plasmids in 293T cells.

***In vitro* kinase assay.** HEK293T cells were transfected with Flag- or Myc-tagged TBK1 plasmid in the absence or presence of HA-YAPs or HA-TAZ plasmid, or transfected with Flag-IRF3 plasmid, and lysed by the modified MLB lysis buffer after 36 h of transfection. Immunoprecipitations were performed by using with anti-Flag, anti-Myc or anti-HA antibodies. With four washes by the MLB and one wash by the kinase assay buffer (20 μM ATP, 20 mM Tris-HCl, 1 mM EGTA, 5 mM $MgCl_2$, 0.02% 2-mercapto-ethanol, 0.03% Brij-35, and 0.2 mg ml^{-1} BSA, pH 7.4), immunoprecipitated Flag- or Myc-tagged TBK1, Flag-IRF3, HA-YAPs, or the GST proteins or GST-tagged wild-type YAP or YAP truncation expressed and purified from *E. coli*, were incubated in the kinase assay buffer at 30 °C for 60 min on a THERMO-SHAKER. The reaction was stopped by the addition of 2 × SDS loading buffer and subjected to SDS–PAGE and specified immunoblotting. Detailed information on the antibodies used in the immunoprecipitation assays is provided in Supplementary Table 2.

Immunofluorescence, microscopy and FACS. To visualize the subcellular localization of endogenous or transfected YAP/TAZ, MAVS or TBK1, NMuMG or HEK293A cells were infected with gVSV virus at 8 hpi, or transfected with the plasmid specified in the results section for 24 h, fixed in 4% paraformaldehyde, permeablized, blocked in 10% horse serum in PBS for 2 h, and incubated sequentially with primary antibodies anti-YAP/TAZ or anti-Flag and Alexa-labelled secondary antibodies with extensive washing. Slides were then mounted with Vectashield and stained with DAPI (Vector Laboratories). Immunofluorescence images were obtained and analysed using the Nikon Eclipse Ti inverted microscope or by the Zeiss LSM710 confocal microscope. FACS analysis of GFP$^+$ cells was performed at BD FACSCalibur, according to the manufacturer's manual. Detailed information for the antibodies used in the immunofluorescence assays is provided in Supplementary Table 2.

CRISPR/Cas9-mediated generation of $YAP^{low}/TAZ^{-/-}$ cells. CRISPR/Cas9 genomic editing for gene deletion was described previously[70]. Guide RNA sequences targeting TAZ (5′-GAGGATTAGGATGCGTCAAG-3′) and YAP (5′-CGGGGAC TCGGAGACCGACT-3′) exons were cloned into the plasmids px330. Constructs together with puromycin vector pCMV-puromycin in the ratio of 15:1 were transfected into NMuMG by PEI transfection reagent. Twenty-four hours after transfection, cells were selected by puromycin (1.5 μg ml^{-1}) for 72 h, and single colonies were obtained by serial dilution and amplification. Clones were identified by immunoblotting with anti-YAP/TAZ antibodies, and the $YAP^{low}/TAZ^{-/-}$ clone was used for the indicated analyses.

Zebrafish ectopic expression and VSV challenge. A system for challenge of GFP-tagged VSV in zebrafish embryos to rapidly assess the gene function in antiviral defence was previously developed[19,20]. Zebrafish AB wild-type embryos (male/female) were raised at 28.5 °C in E3 egg water. Forced expression of exogenous genes GFP or YAP 6SA was obtained by microinjection of 25 pg of *in vitro*-transcribed mRNA by the mMESSAGE mMACHINE SP6 Transcription Kit (Life technology) into the one-cell stage of embryogenesis, that is, the first 20 min. At this stage, exogenous mRNAs distribute most evenly into most cells by cell division and last for 72–96 h in zebrafish embryos. Injected embryos with normal development were selected and used for the gVSV virus microinjection (1×10^3 pfu per embryo) at the embryo yolk at 48 hpf, and a simple randomization method was used for allocation groups. The infection and death rate of injected embryos were monitored at desired stages. To detect the expression of GFP or YAP 6SA by immunoblotting, tissue samples of zebrafish embryos at 48 hpf were homogenized, lysed in MLB, and subjected to SDS–PAGE and immunoblotting. To detect the expression of zebrafish

DOI: 10.1038/ncb3496

IFNs and ISGs in response to gVSV infection, tissue samples of zebrafish embryos at 24 hpi were homogenized and lysed, and subjected to RNA extraction and qRT–PCR assays as described in the previous section. Care of experimental animals was in accordance with guidelines and approved by the laboratory animal committee of Zhejiang University.

Statistics and reproducibility. Quantitative data are presented as mean ± standard error of mean (s.e.m.) from at least three independent experiments. When appropriate, statistical differences between multiple comparisons were analysed using the ANOVA test with Bonferroni correction, and the survival curve was analysed using the log rank test, both by Origin 9.1 software. Differences were considered significant at $P < 0.05$ and the P value was precisely specified unless it is smaller than 0.001. All samples if preserved and properly processed were included in the analyses, and no samples or animals were excluded, except for zebrafish with conventional injection damage. No statistical method was used to predetermine sample size, and the experiments except for animal samples were not randomized. Immunoblottings, for which representative experiments are shown in the figures, as well as reporter assay, and qRT–PCR experiments were repeated to a minimum of three independent experiments to ensure reproducibility. The investigators were not blinded to allocation during experiments and outcome assessment.

Data availability. All data supporting the findings of this study are available from the corresponding author on reasonable request. The source data for statistical analyses of Figs 1a,c–e,g, 2a–c,f,h, 3a,b, 5b, 6d,e and 8b,c and Supplementary Figs 1A, 2A–C,E,F, 4B and 5B are provided in Supplementary Table 1.

69. Xu, P. *et al.* Innate antiviral host defense attenuates TGF-β function through IRF3-mediated suppression of Smad signaling. *Mol. Cell* **56,** 723–737 (2014).
70. Ran, F. A. *et al.* Genome engineering using the CRISPR-Cas9 system. *Nat. Protoc.* **8,** 2281–2308 (2013).

nature cell biology

DOI: 10.1038/ncb3496

In the format provided by the authors and unedited.

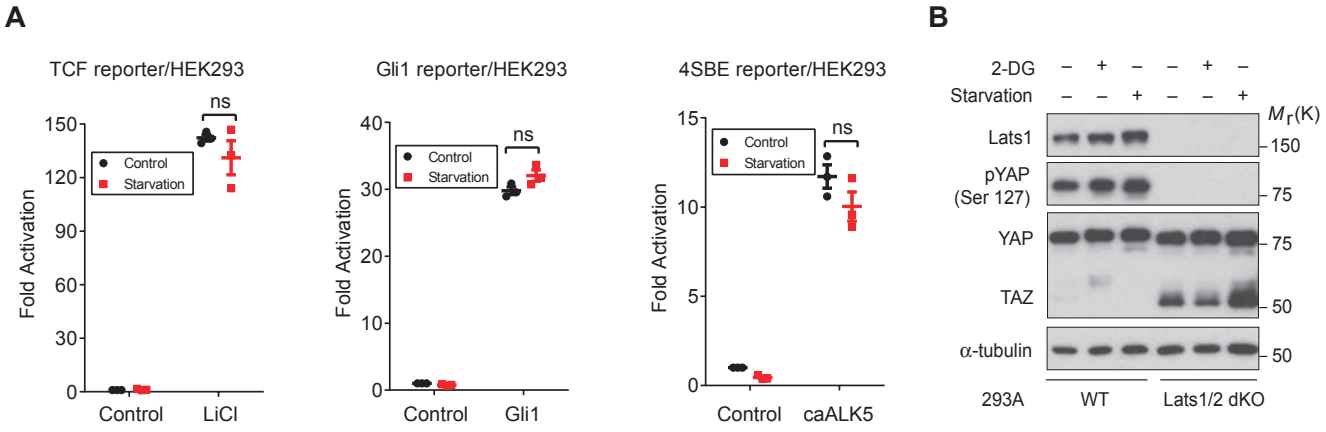

Supplementary Figure 1 The responses of Lats1/2 dKO cells and other signaling pathways to energy/nutrient stress. Related to Figure 1. (A), Serum starvation failed to significantly potentiate the Wnt, Hedgehog, and TGF-β/Smad signaling, measured by indicated reporters and stimulated by LiCl treatment, Gli1, or activated type I TGF-β receptor, respectively. n=3 independent experiments. Mean ± SEM. P>0.05, by ANOVA test and Bonferroni correction. (B), Lats1/2 dKO HEK293A cells did not respond to glucose stress (2-DG treatment) or nutrient stress (serum starvation) to activate YAP Ser127 phosphorylation or to cause TAZ degradation. Unprocessed images of blots are shown in Supplementary Figure 6. Statistics source data are provided in Supplementary Table 1.

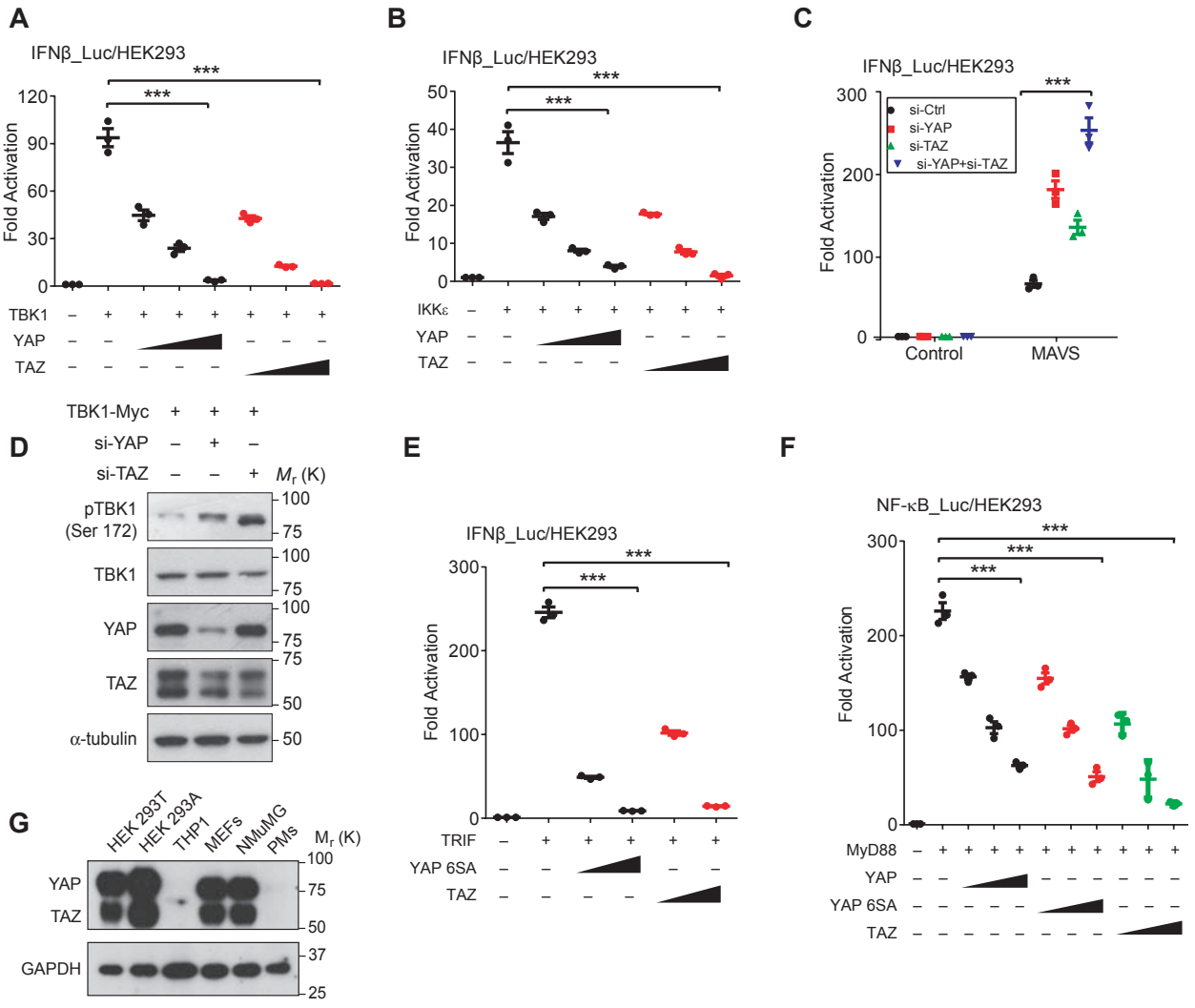

Supplementary Figure 2 YAP/TAZ inhibit signaling pathways mediated by MAVS, TBK1, TRIF and MyD88. Related to Figure 2. (A) and (B): Ectopic expression of YAP or TAZ inhibited IRF3 transactivation that was stimulated by TBK1 (A) or IKKe (B), in a dose-dependent manner. n=3 independent experiments. ***P<0.001, by ANOVA test and Bonferroni correction. (C), IRF3 transactivation stimulated by MAVS was also boosted under siRNA-mediated depletion of YAP and/or TAZ. n=3 independent experiments. Mean ± SEM. ***P<0.001, by ANOVA test and Bonferroni correction. (D), siRNA-mediated knockdown of YAP or TAZ enhanced the activation of ectopically expressed TBK1. (E) and (F), Coexpression of YAP 6SA or TAZ suppressed the IRF3 responsiveness stimulated by TRIF cotransfection (E), or the NF-κB responsiveness stimulated by MyD88 cotransfection (F). n=3 independent experiments. Mean ± SEM. ***P<0.001, by ANOVA test and Bonferroni correction. (G), Endogenous YAP/TAZ proteins were abundant in HEK293, mouse embryonic fibroblasts (MEFs) and NMuMG epithelial cells, but were scarce in THP-1 monocytes and peritoneal macrophages (PMs). Unprocessed images of blots are shown in Supplementary Figure 6. Statistics source data are provided in Supplementary Table 1.

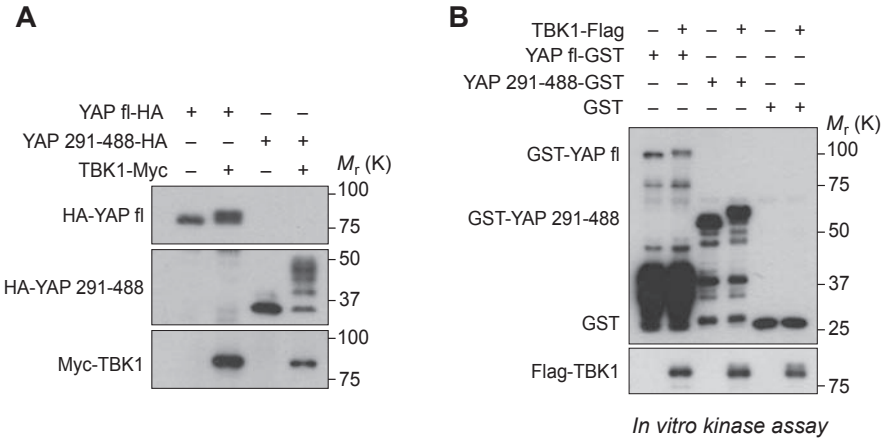

Supplementary Figure 3 TBK1 modifies full-length and the transactivation domain of YAP in cells and *in vitro*. Related to Figure 5. (A) and (B), TBK1-mediated modification of full-length (fl) or the transactivation domain (a.a. 291-488) of YAP was revealed by the evidently mobility shift of YAPs, occurred during coexpression in cells (A), or during an *in vitro* kinase assay with GST tagged YAPs expressed and purified from *E.coli*. Unprocessed images of blots are shown in Supplementary Figure 6.

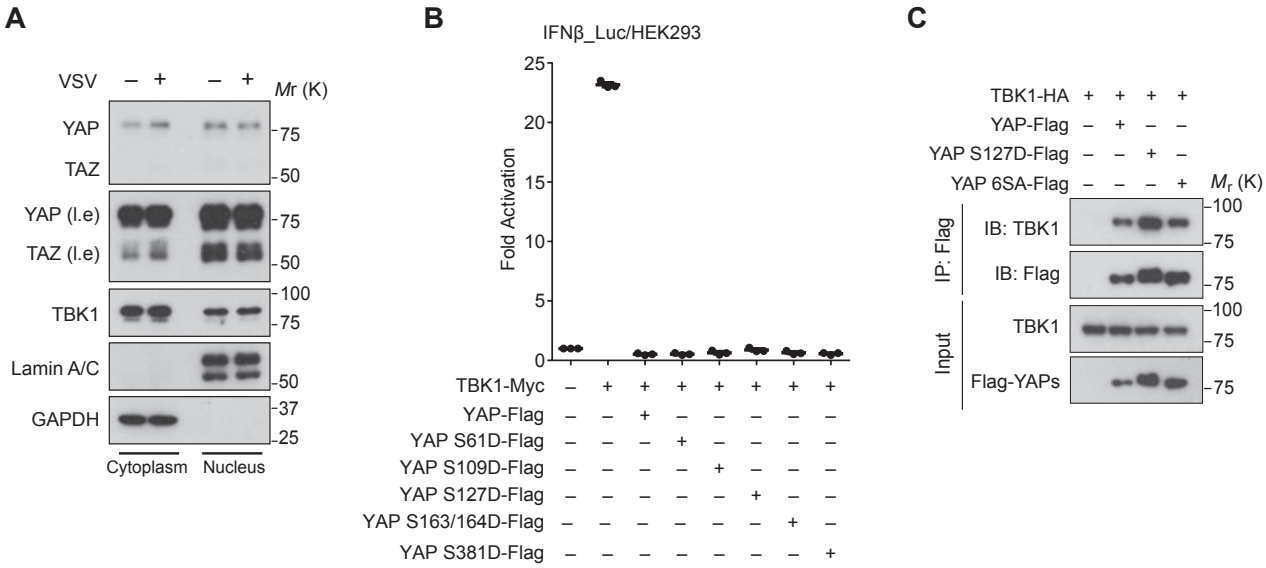

Supplementary Figure 4 VSV-induced translocation and TBK1 association of YAP/TAZ. Related to Figure 6. (A), VSV infection induced a translocation of endogenous YAP/TAZ from the nucleus to the cytoplasm in HaCaT cells, revealed by the nuclear/cytoplasmic fractionation and subsequent immunoblotting. (B), Individual mutations of five Serines (Ser61, Ser109, Ser127, Ser164, or Ser381) into Aspartate did not release YAP's inhibition on TBK1 substantially. n=3 independent experiments. Mean ± SEM. (C), Interactions between TBK1 and YAP 6SA or YAP mimetic with Ser127 phosphorylation was revealed by co-immunoprecipitation. Unprocessed images of blots are shown in Supplementary Figure 6. Statistics source data are provided in Supplementary Table 1.

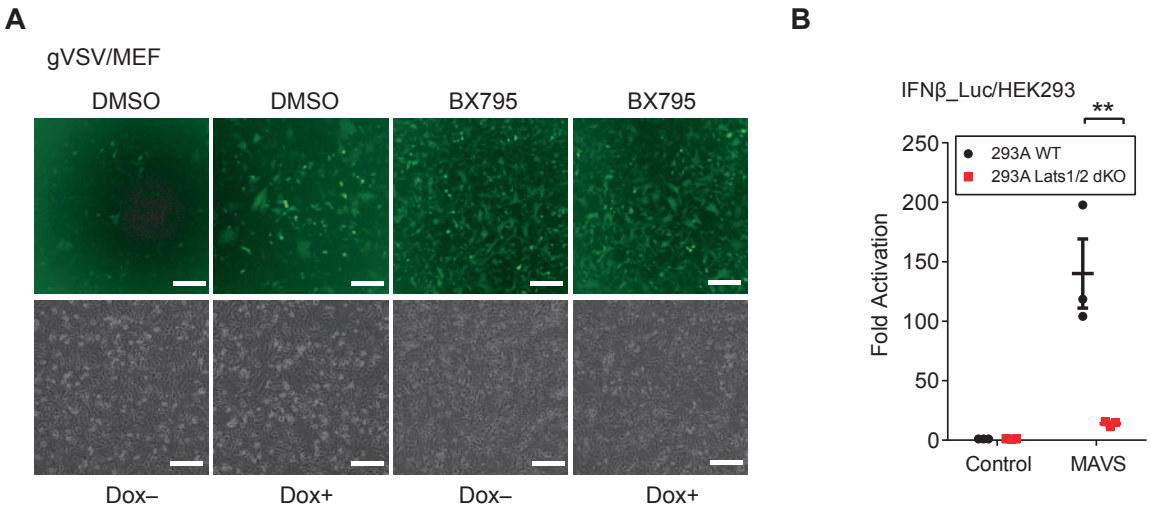

Supplementary Figure 5 YAP and Lats1/2 are involved in regulation of antiviral signaling and resistance. Related to Figure 7. (A), Treatment of the TBK1/IKKε inhibitor BX795 eliminated most inhibitory effect of YAP 6SA on antiviral defense, suggesting that this regulation is mainly through TBK1/IKKε. Scale bars, 100 μm. (B), Decreased levels of antiviral signaling stimulated by MAVS coexpression was observed in Lats1/2 dKO HEK293A cells by the IRF3-responsive reporter assay. n=3 independent experiments. Mean ± SEM. **P=0.0017, by ANOVA test and Bonferroni correction. Unprocessed images of blots are shown in Supplementary Figure 6. Statistics source data are provided in Supplementary Table 1.

Figure 1

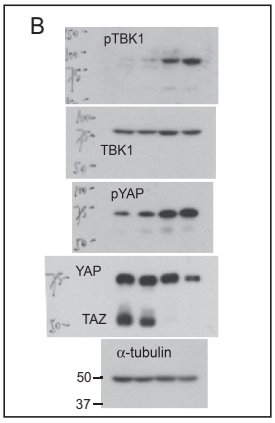

Figure 1

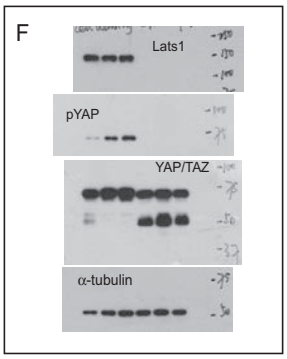

Figure 1

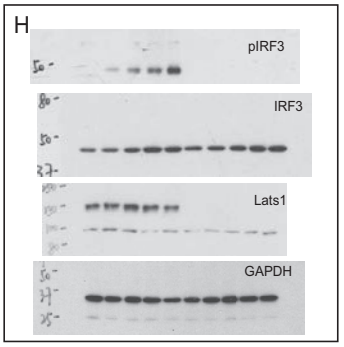

Figure 2

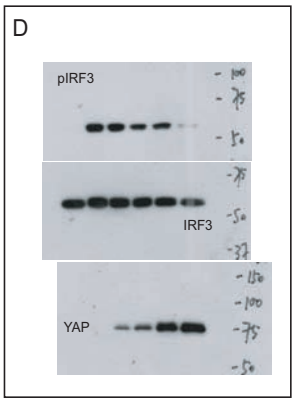

Figure 2

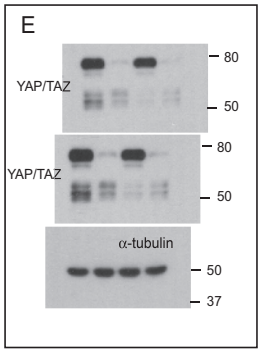

Figure 2

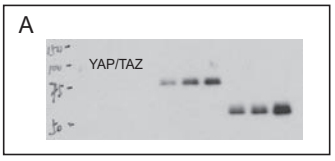

Figure 3

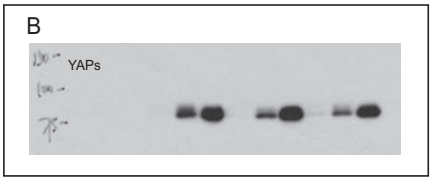

Figure 2

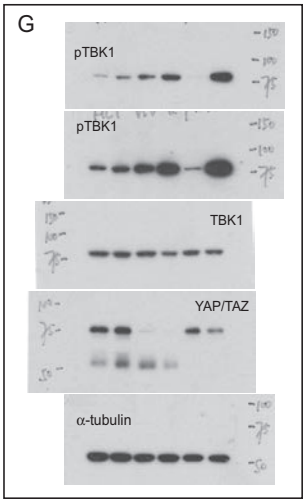

Figure 2

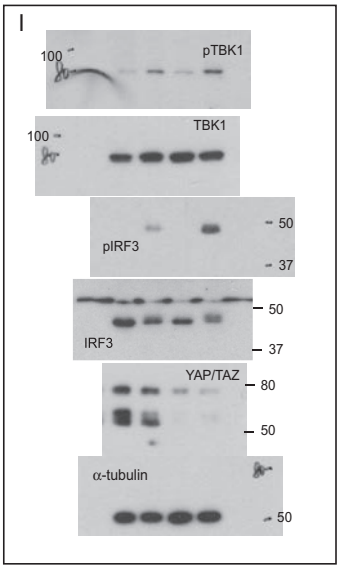

Figure 3

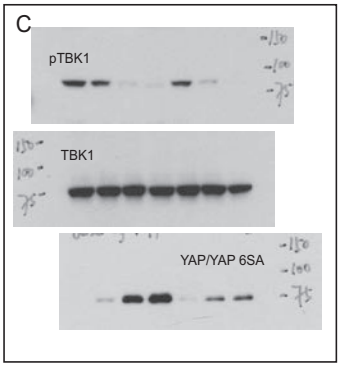

Supplementary Figure 6 Unprocessed images of blots. Unprocessed images of scanned immunoblots shown in Figures and Supplementary Figures are provided.

Figure 3

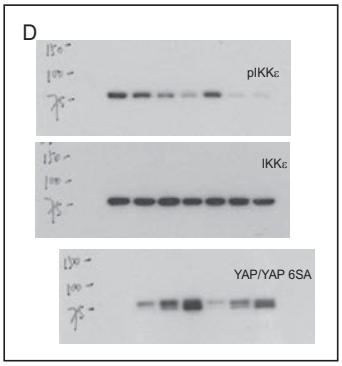

Figure 3

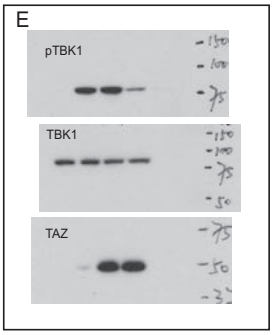

Figure 3

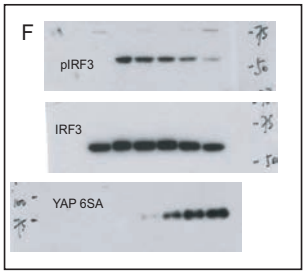

Figure 3

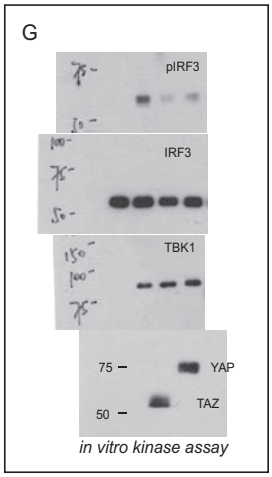

Figure 4

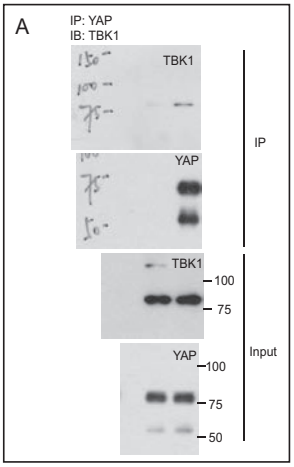

Figure 4

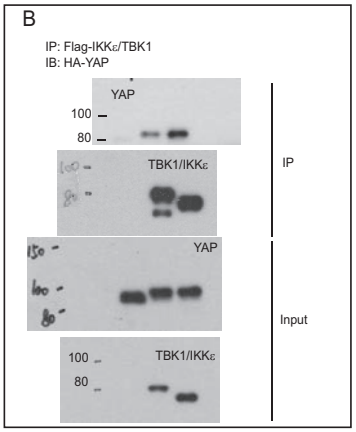

Figure 4

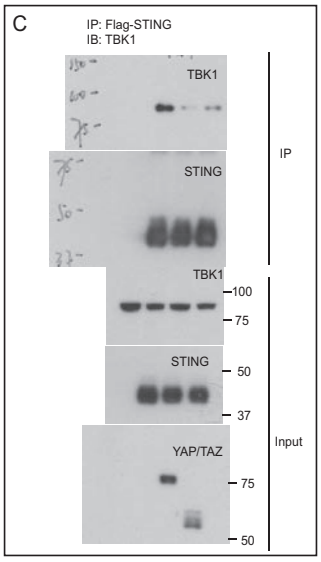

Figure 4

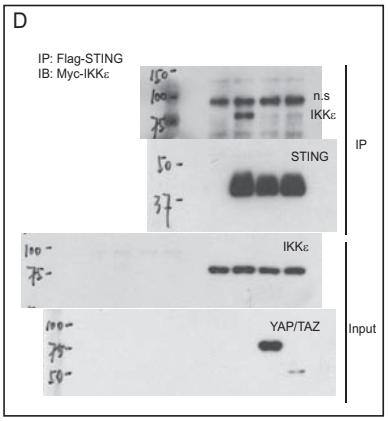

Figure 4

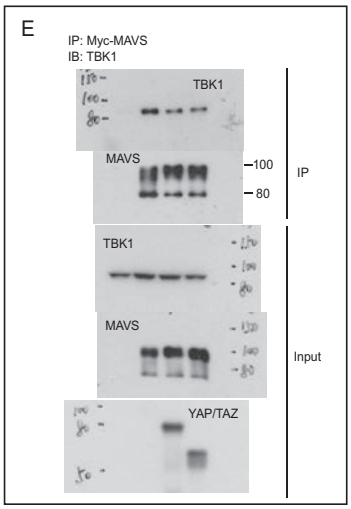

Supplementary Figure 6 Continued

Figure 4

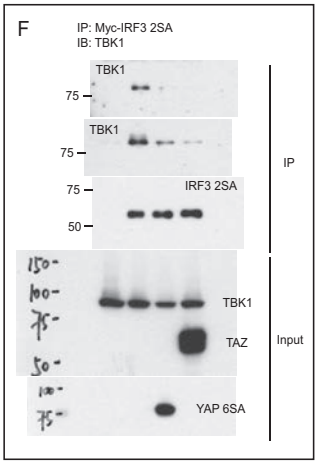

Figure 4

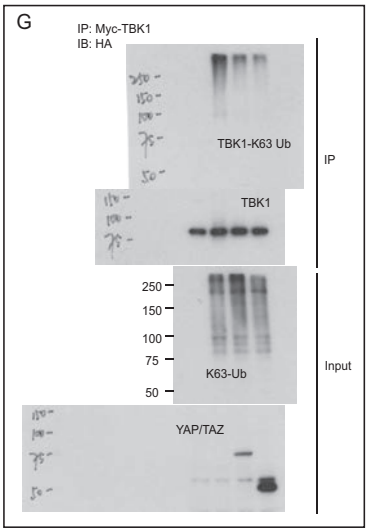

Figure 4

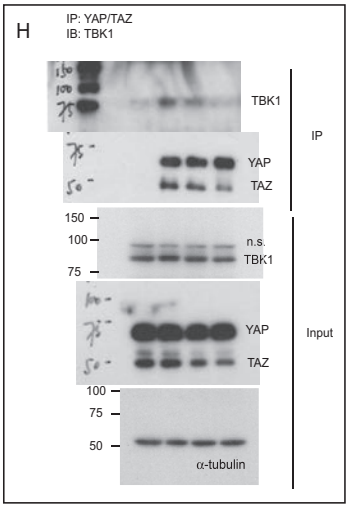

Figure 4

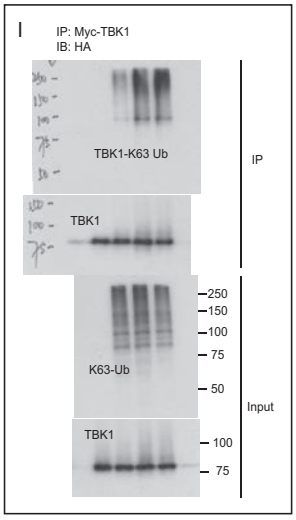

Figure 5

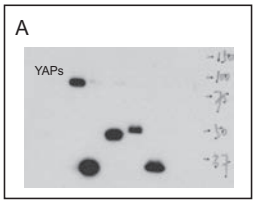

Figure 5

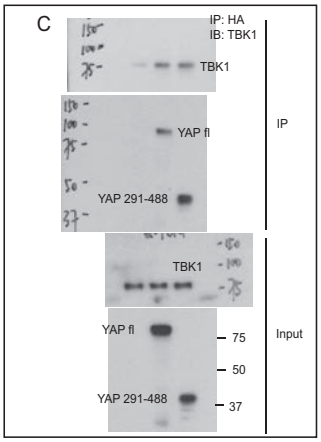

Figure 5

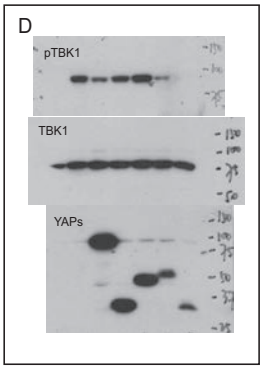

Figure 5

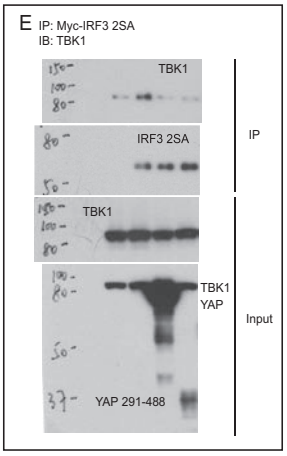

Figure 5

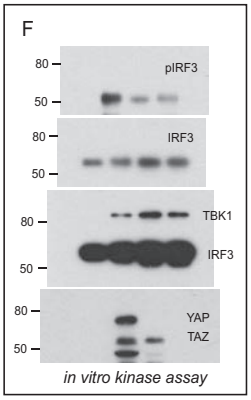

Supplementary Figure 6 Continued

Figure 5

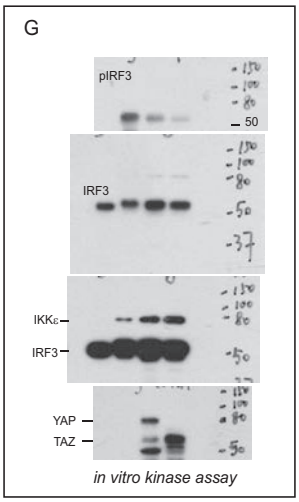

Figure 5

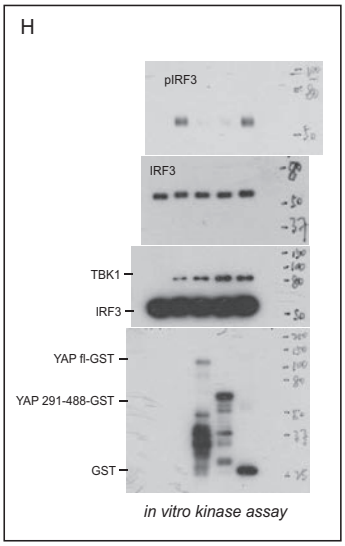

Figure 6

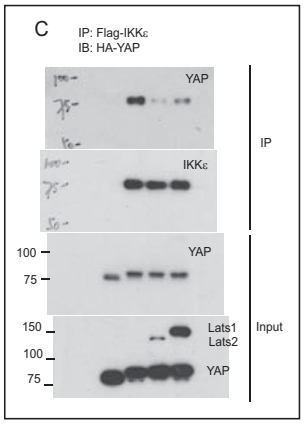

Suppl. Figure 1B

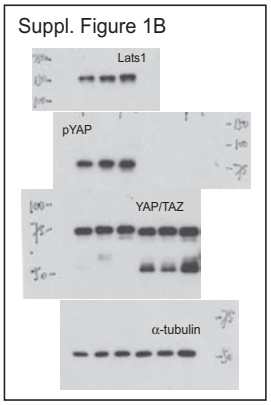

Figure 7

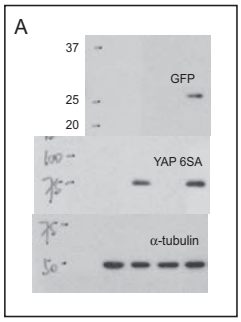

Figure 7

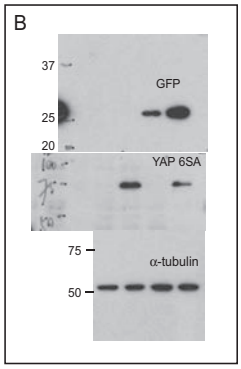

Figure 8

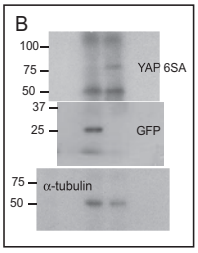

Suppl. Figure 3B

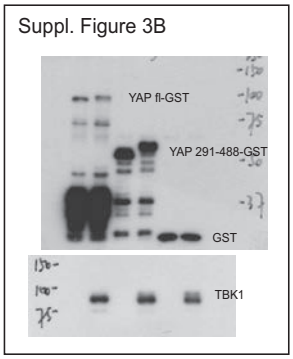

Suppl. Figure 2G

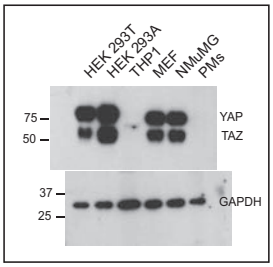

Suppl. Figure 4A

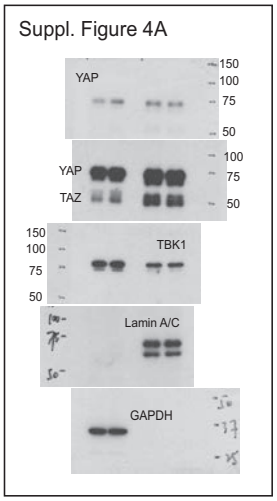

Suppl. Figure 2D

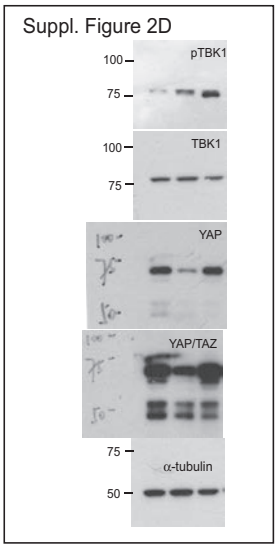

Suppl. Figure 3A

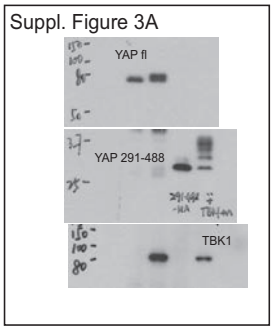

Suppl. Figure 4B

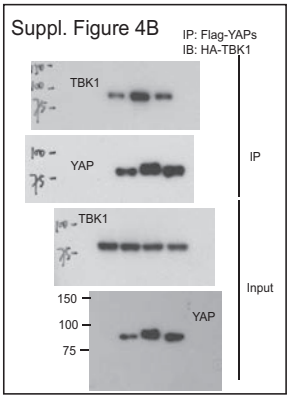

Supplementary Figure 6 Continued

Supplementary Table Legends

Supplementary Table 1 Statistics Source Data. The source data used for statistical analyses of Figures 1A, 1C, 1D, 1E, 1G, 2A, 2B, 2C, 2F, 2H, 3A, 3B, 5B, 6D, 6E, 8B and 8C, and Supplementary Figures 1A, 2A, 2B, 2C, 2E, 2F, 4B and 5B are provided.

Supplementary Table 2 Information of antibodies. The detailed information of antibodies in distinct applications is provided, including sources, catalog numbers, and dilutions.

Supplementary Table 3 Sequence and information for RNAi and primers used for qRT-PCR. The nucleotide sequences or information of RNAi, and individual primers used for qRT-PCR to quantitate both human and zebrafish mRNA levels are provided.